+

Faculty of Science and Engineering

School of Chemical and Physical Science

Master Thesis – Master Student

Project Title: Synthesis of Molybdenum Disulfide, and Preparation of Hybrid Molybdenum Disulfide/Single Wall Carbon Nanotubes–n-type Silicon Solar Cells

Student name: Samira Salem Almalki

Student FAN: alma0173

Student ID: 2132672

Supervised by: Professor. Joe Shapter

Submitted on: 09 November 2016

Declaration

I Samira Salem Almalki hereby declare that this thesis is my original work. Otherwise, contributions from others are acknowledged and referenced (literature). This project work was done under Professor Joe Shapter's supervision.

Samira Salem Almalki

09 November 2016

alma0173@flinders.edu.au

Samira
Almalki

Acknowledgment

At first I gratefully would like to express my deep thanks to the Saudi Cultural Mission for their financial funding and ultimate support. My genuine appreciation goes to my supervisor Professor Joe Shapter, who constantly and patiently provides me with his advice, suggestions, and support during my Master's project. Without his persistent encouragement and guidance I would not be able to pursue my lab work and thesis writing. I would also like to thank Joe's group members; Dr. Cameron, PhD candidate Munkhbayar Batmunkh, PhD candidate Tom Grace, Masters candidate Munkhjargal Bat-Erdene, for their useful advice, suggestions, answering my questions, helping in the lab, providing the laboratory's resources. Similarly, Dr. Mahnaz Dadkhah Jazi for both the glove box and the new mask training, Dr. Ashley Slattery for both the Raman Spectroscopy and Scanning Electron Microscopy (SEM) training. Likewise, Dr. David Vincent for both the HF etching and UV-Visible Spectroscopy training, and Dr. Christopher Gibson for the Atomic Force Microscopy (AFM) training. Deepest thanks to PhD candidate Leping Yu for the training on the solar cells preparation, the Solar Simulator, and the 4-Point Probe training. Special thanks and gratefulness to my parents, who continuously pray for me. Besides, my husband who spiritually supported me during my Masters study, my son and friends. Additionally, I wish to acknowledge the Australian Microscopy & Microanalysis Research Facility (AMMRF) for all instruments including the AFM, SEM, Raman and glove box.

Table of Contents

Abstract

Molybdenum disulfide (MoS_2) is a two-dimensional material from the layered transition-metal dichalcogenides semiconductor family (LTMDs), which involves two hexagonal layers of sulfur (S) and an intermediate hexagonal layer of molybdenum (Mo). MoS_2 has a band gap structure that is sensitive to strain and also has high carrier mobility. The band gap's nature changes from indirect to direct in single monolayers associated with the decrease in the material thickness. The chemical exfoliation of the MoS_2 to form single monolayers will activate its optical properties and allows its use in innovative devices. Therefore, combining MoS_2 and CNTs will provide novel photovoltaic devices. In this study, molybdenum disulfide is exfoliated using lithium intercalation, which is then characterised using AFM, SEM, and Raman. The MoS_2 layer thickness was ~1-100 nm while the flake's lateral dimensions range from ~100-500 nm. From Raman spectrum the MoS_2 characteristic peaks emerge at ~385 cm^{-1} and ~405 cm^{-1} which correspond to E^1_{2g}, and A_{1g} vibrations modes respectively. The purpose of this research is to use the molybdenum disulfide in SWCNTs-n-type silicon based solar cells. This addition enhanced the solar cell efficiencies from ~7 % for CNT-Si cells to ~10 % for MoS_2/CNT-n-Si cells.

Chapter 1: Introduction

Solar cells

The most important thing to provide the next generation is energy sustainability. The sun's rays are abundant and can provide more energy than the current daily consumption and even the future's needs. Solar power is the most sustainable renewable energy to provide. With this sort of energy, where it depends on a renewable energy source, there would be no greenhouse gas emissions. Also, utilising the sun's irradiances can eliminate the lost energy due to the distribution grid which in fact accounts for almost 25% of produced electricity being lost.[1] The consumption of fossil fuels can be reduced with solar energy and also, other harmful energy sources that lead to pollution and crisis in the environment can be used less.[2] A solar cell's working principle relies on three elements, the light adsorption that creates a charge carrier (electrons as n-type and holes as p-type), followed by the charge carrier separation due to a difference in the potential at the p-n junctions. Finally, the charge carrier collection occurs at the respective electrodes. Photovoltaics is one of the fastest growing optoelectronic applications.[3] There has been huge interest from researchers in developing solar energy in recent years especially when using 2D material with optimal properties. For instance, molybdenum disulfide (MoS_2) has distinctive optical, photodetection, and electronic characteristics.[4] Although, recent solar cells are developing tremendously some of them still have downsides to overcome. There are three crucial negatives: the difficulty in terms of manufacturing process, the high expense of solar cells and the electrical properties they have which limit the cell's efficiencies.[5] In this research attaching a layer of molybdenum disulfide (MoS_2) that hybridises with carbon nanotubes (SWCNTs) which is then applied to n-type silicon solar cells will maximise electricity generation. Moreover, at the same time this will produce cost effective solar cells, optimal charge collection, optimise the separation of the charge carriers and create better performing photovoltaics.

Carbon Nanotubes-n type Silicon Solar Cells

There are many materials that are used in fabricating photovoltaics but most of them have many problems such as toxicity, short lifetimes, some transmission drawbacks and high cost. Silicon solar cells have a high cost of production since silicon is costly; they are also inflexible and heavy. Accordingly, the solution is using alternative materials to overcome most of these downsides. As CNTs have outstanding characteristics and are plentiful this makes them promising candidates for solar cells. CNTs have really low-cost in large-scale production, are strong, have high chemical, thermal and photo stability, extreme conductivity, as well as excellent electrical and optical characteristics.[1,5-7] Carbon in the form of nanotubes is utilised in silicon solar cells photovoltaics. There are two possible mechanisms when using SWCNTs

to convert the light into electricity 1) use the SWCNTs as a transparent electrode in the metal semiconducting Schottky junction solar cells or 2) in heterojunction solar cells where the SWCNTs' role is as a photoactive material.[8] There are two sorts of single walled carbon nanotubes, namely semiconducting and metallic which depend on the diameter, and the hexagon ring arrangement.[9] There are remarkable differences between the two types. The device is fabricated using two materials namely the n-type silicon solar cells and p-type single walled carbon nanotube thin films[1] as shown in Figure (1).

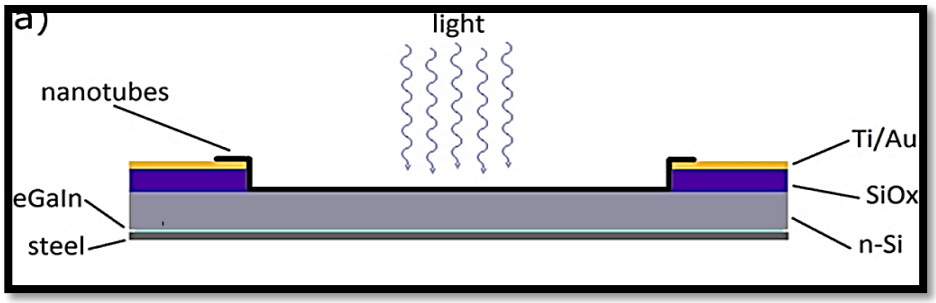

Figure (1): SWCNTs-n type Silicon solar cell device.[10]

These sort of solar cells yield an efficiency of 14%.[11] Herein, the SWCNTs thin films are deposited on the n-type doped silicon substrates in order to generate a photoactive junction. The role of CNT film is to act as the transparent electrode to harvest the light.[8,11] There are two principal factors which affect the SWCNTs-silicon cell's performance, the transparency and the conductivity of the CNT layer.[10] In this device, a depletion region is created at the interface between the n-type silicon and the p-type SWCNTs. [8] The p-n heterojunction solar cells' mechanism is the following: (see Figure (2)).

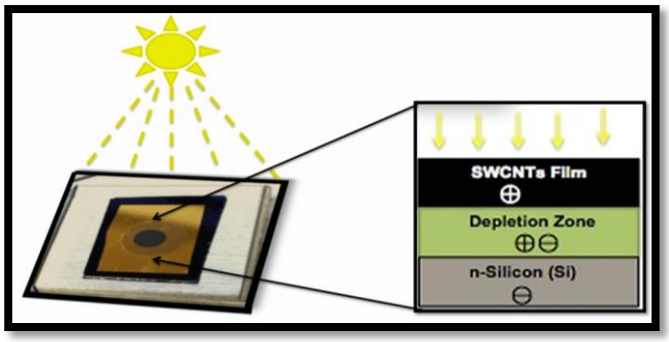

Figure (2): How does the solar cell work?

As shining the light the n-type silicon material absorbs the photons, where, the single walled carbon nanotubes material act as the p-type semiconductor that transports holes. Then, the excitons are created which can diffuse to the depletion region. Later, when they are in the depletion region, they separate into free charges as a result of the created potential because of the energy variances. Finally, the holes are transported thorough the SWCNTs films and

the electrons through the silicon substrate to be able to extract into the exterior circuits and this is what creates the electricity as shown in Figure (3)[11,12]

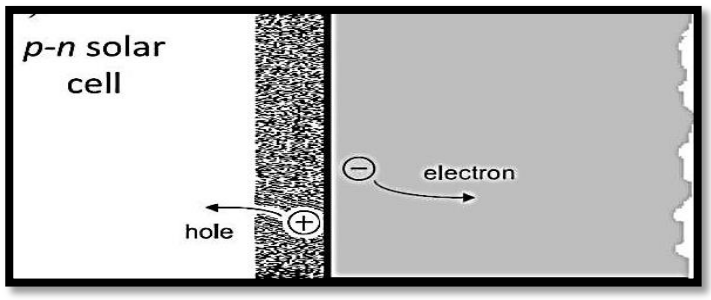

Figure (3): A schematic for CNTs-n-Silicon solar cells (p-n solar cells).[11]

Molybdenum Disulfide (MoS_2)

Molybdenum disulfide (MoS_2) is a two-dimensional semiconductor material and from the archetypal transition metal dichalcogenide (TMDs) materials.[13] MoS_2 is a solid-state catalyst and lubricant especially in the hydrogen evolution process. A monolayer (1L-MoS_2) contains of two hexagonal sulfur sheets (S) and in-between them is the hexagonal sheet of molybdenum (Mo) as shown in Figure (4 a, b, and c). They interact with each other by covalent bonds through a sequence of S-Mo-S where the layers are held together via van der Waals forces.[14-17]

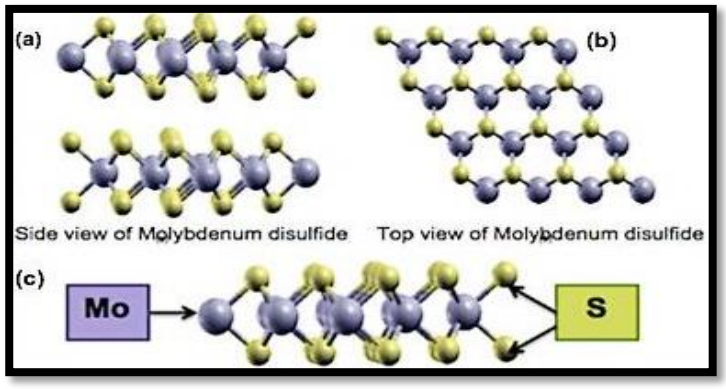

Figure (4): a) Structure of bulk MoS_2 from side view, b) Structure of monolayer and bulk MoS_2 from top view, c) Structure of monolayer MoS_2 from side view.[18]

Molybdenum disulfide is an interesting material among the 2D materials for an intriguing range of applications; photovoltaics, sensors, photodetectors, and lithium ion batteries.[14,15] Scientists attempt to switch to MoS_2 rather than graphene because MoS_2 stands out with innovative characteristics. Those are correlated with its ultrathin nano-sized sheets. Certainly, these ultimate properties put the MoS_2 in the list as a perfect candidate for the next generation of the solar cells industry whilst, graphene has revealed some limitations such as a weak band gap.[19,20] The bulk form of MoS_2 has indirect band gap semiconductor (energy gap 1.2eV) where, the single layers of MoS_2 has a direct band gap (energy gap 1.9eV) as shown in Figure (5).

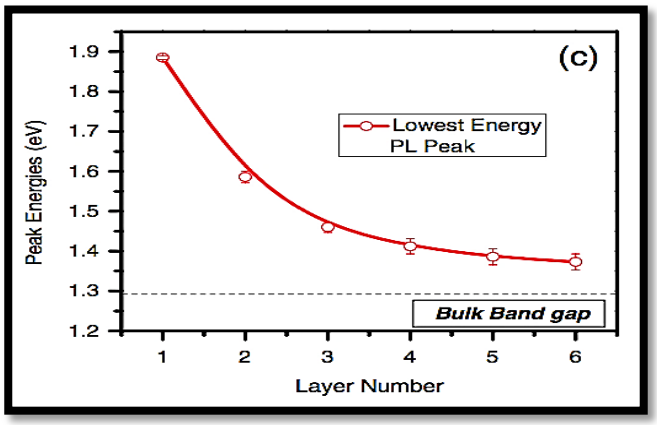

Figure (5): The MoS_2 band gap energy for single and multilayers.[21]

Lithium intercalation and Chemically exfoliation the Molybdenum Disulfide (MoS_2)

In order to pursue this research project chemical exfoliation of the bulk MoS_2 to single monolayer via the lithium intercalation (Li_xMoS_2) will activate the MoS_2 optical properties and reveal its tuneable direct band gap. Then, the 2D material can be implemented in innovative devices.[21] Indeed, lithium intercalation is considered one of the easiest techniques to synthesise monolayers of MoS_2. Lithium intercalated the molybdenum disulfide (Li_xMoS_2) produces a scalable and stable colloidal suspension with sheet thickness of (3-12nm) for (5-20) monolayers. The exfoliation of MoS_2 into monolayers is done, when inserting the lithium between the MoS_2 layers. At this stage both the lithium and water react with each other and form hydrogen gas at the boundary which, when used with the ultrasonication, yields fabrication of water dispersed chemically exfoliated molybdenum disulfide layers as shown in Figure (6).[14,15,22]

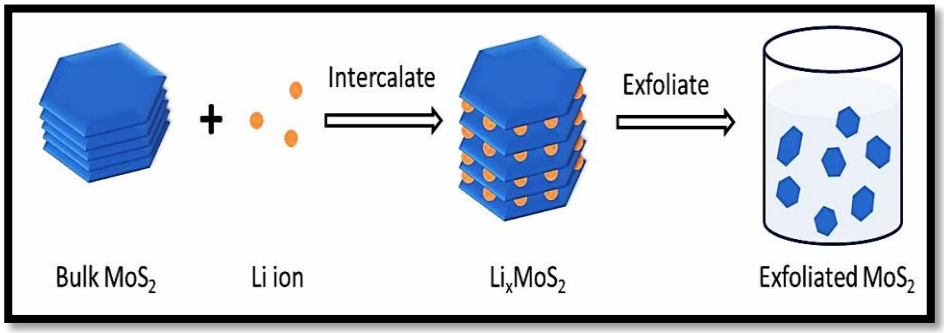

Figure (6): The chemically exfoliation procedure of MoS_2.[23]

MoS_2 is simply cleaved because of the weak van der Waals forces, which exist between the layers. Varying MoS_2 band gap's nature from indirect to direct transition will increase the photoluminescence quantum yield by (10^4) which distinguishes the MoS_2 monolayer from multilayer. MoS_2 is used as electron acceptor, with robust mechanical characteristics, that indicate MoS_2, can be applied in optoelectronic devices, flexible field effect transistors, and photodetectors particularly as a monolayer. The use of MoS_2 in organic solar cells reported

an efficiency of ~7.6%.[15,22] Definitely, MoS_2 has poor electron transport since; MoS_2 has a semiconducting 2H phase and metallic 1T phase see Figure (7).

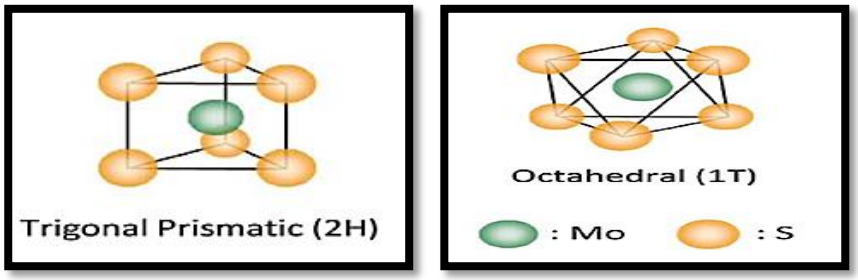

Figure (7): The MoS_2 semiconducting (2H) and metallic (1T) phases.[22]

In fact, the semiconducting 2H phase restricts the MoS_2 conductivity, which can be overcome by utilising CNTs that have high conductivity. Furthermore, the SWCNTs have a difficulty with charge carrier hopping between the CNTs. The addition of MoS_2 will solve the carrier density barrier since it has a long carrier diffusion length (200-500cm^2/Vs) so as a result MoS_2 can transport the holes easily instead of having the charge carriers hopping from one tube to another. The addition of MoS_2 will reduce the number of charge carrier hops between the CNTs which will enhance the solar cell's efficiency.[22,24]

Project aims

Thus, in this research project, after preparing the molybdenum disulfide single layer films, the CNTs suspension and hybridised MoS_2 with SWCNTs. The objective is to fabricate thin film solar cells where the n-type semiconductor is the n-type silicon and the p-type semiconductor is the SWCNTs. Then the molybdenum disulfide will be added as an n-type semiconductor to the CNTs-Si based solar cells. This fabrication will result in new device design MoS_2/SWCNTs-n-type Si solar cells. These combinations will solve the device's efficiency and high cost of fabrication. Hence, hybridising the MoS_2 and CNTs will provide novel photovoltaic devices (see Figure (8)).

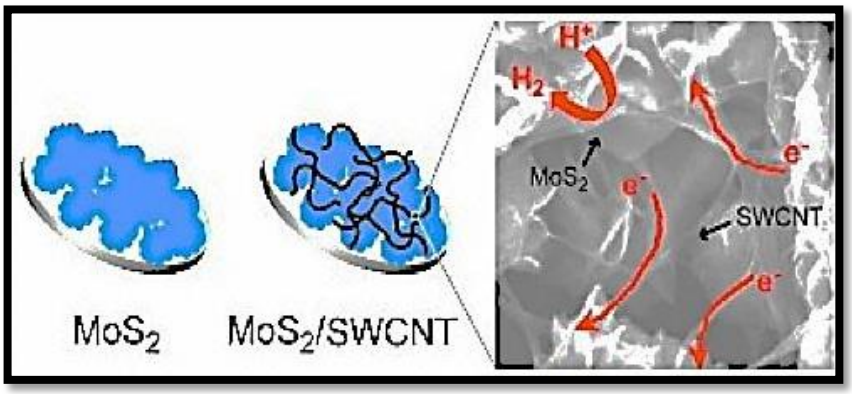

Figure (8): The hybrid MoS_2 with SWCNTs process.[25]

As a result of that, the key intention of this research project is to fabricate three novel high-performance solar cells, see Figures (9), (10) and (11); the first one is the single wall carbon nanotubes n-type silicon based solar cells. The second type is the hybrid MoS_2/SWCNTs-n-type Si solar cells which done by filtering different volumes of MoS_2 (100-2000µL) and CNTs at the same time with a control volume of SWCNTs (300µL). While the third type is the layered MoS_2/SWCNTs-n-type Si solar cells, where first the MoS_2 film is attached and then another SWCNTs film is attached over the MoS_2 film, which done by filtering different volumes of MoS_2 (100-1000µL) and then at the same time filtering another layer with control volume of SWCNTs (300µL) via vacuum filtration method. Once made, a comparison of the second and third solar cells' efficiencies and SWCNTs-n-type Si based solar cells' efficiency was obtained.

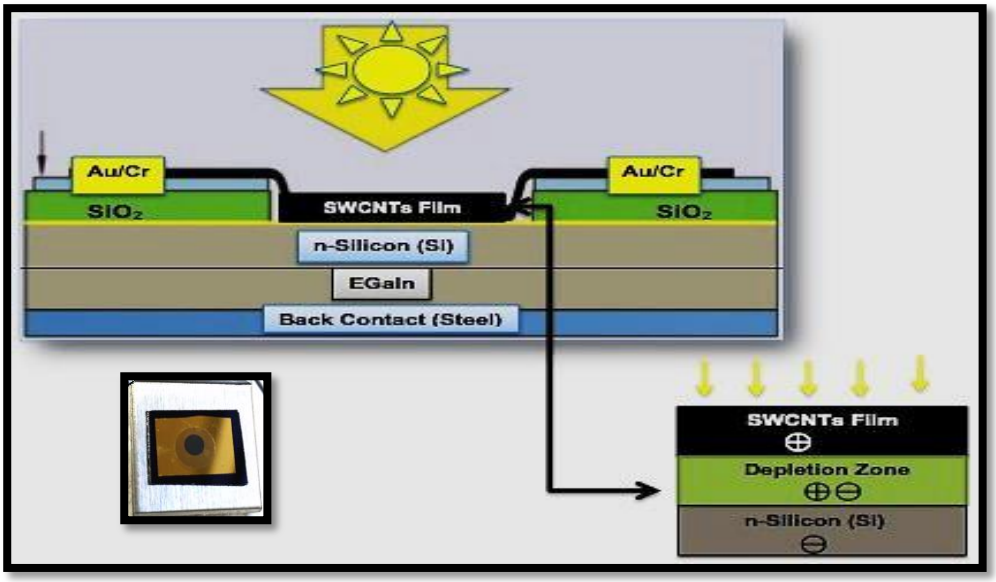

Figure (9): A schematic structure for the pristine SWCNTs-n-Si solar cell.[26]

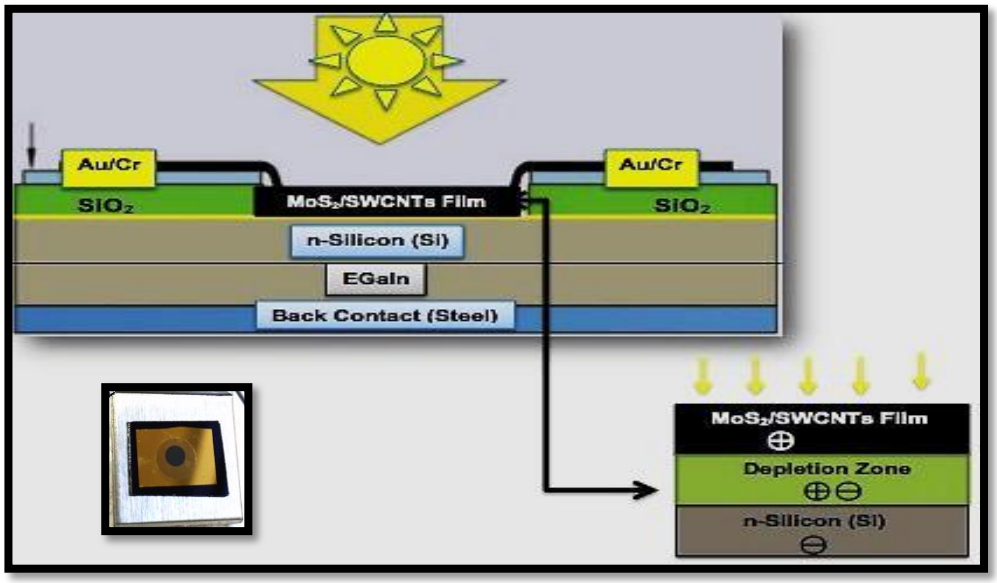

Figure (10): A schematic structure for the hybrid MoS_2/SWCNTs-n-Si solar cells.[26]

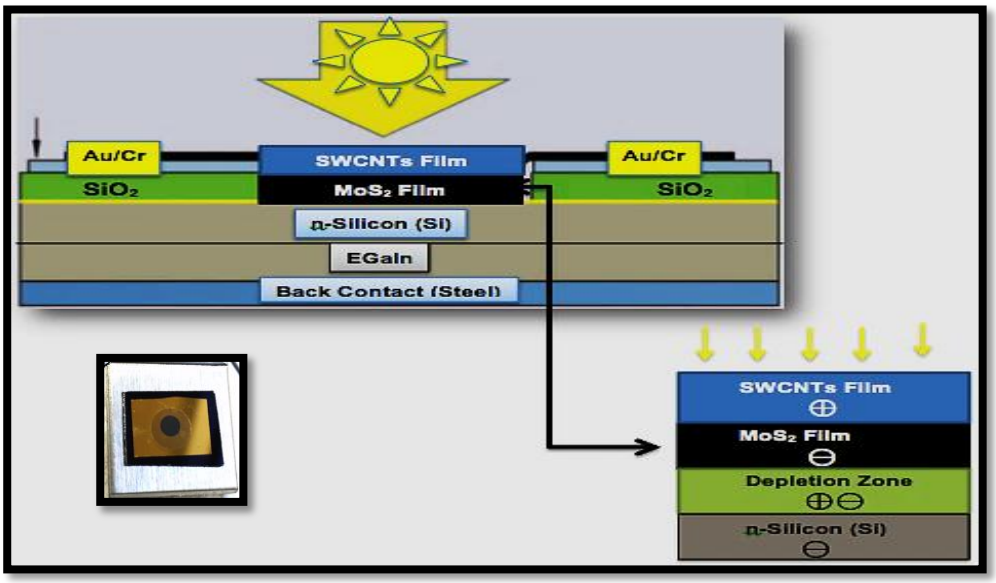

Figure (11): A schematic structure for the layered MoS_2/SWCNTs-n-Si solar cells.[26]

Chapter 2: Experimental details /Theoretical methods

Preparing the solutions

Lithium intercalation and Chemically exfoliation single layers of Molybdenum Disulfide

In this research project, the first step was the preparation of a single or few layer molybdenum disulfide colloidal suspensions from the MoS_2 crystals through the Li intercalation inside a glove box that was filled with nitrogen gas. Roughly 0.2g of 2D molybdenum disulfide crystals (FlexeGRAPH) was mixed with 0.2mL of n-butylithium solution 20 M in cyclohexane (Sigma Aldrich) in order to achieve the lithium intercalation. Next, after the exfoliation was achieved, the (Li_xMoS_2) was filtered using 60mL of hexane (Chem-supply) through vacuum filtration to get rid of the solid lithium and other unwanted organics. After that, the exfoliation was completed within 30minutes using bath sonication of the Li_xMoS_2 for around 1hour in 50mL-deionised water. Then, the solution was centrifuged two times in order to remove the lithium in the form of lithium hydroxide (LiOH) and other unexfoliated materials. The first centrifuge was completed under slow speed centrifugation (4000rmp at 7g for 30minutes). This was to get rid of the unexfoliated particles, in this case, the supernatant was kept and the precipitate was discarded. The second centrifuge was done under high-speed centrifugation (17.000rmp at 7g for 1hour). This was to eliminate any lithium ions. Thus, the exfoliated particles (the precipitate) were collected and the liquid, which contains the lithium ions, was discarded. Finally, adding 50mL of fresh water produced an ultrapure colloidal suspension of molybdenum disulfide. Figures (12a and b) show how the solution colour was black after bath sonication and after centrifugation changed to dark yellow.

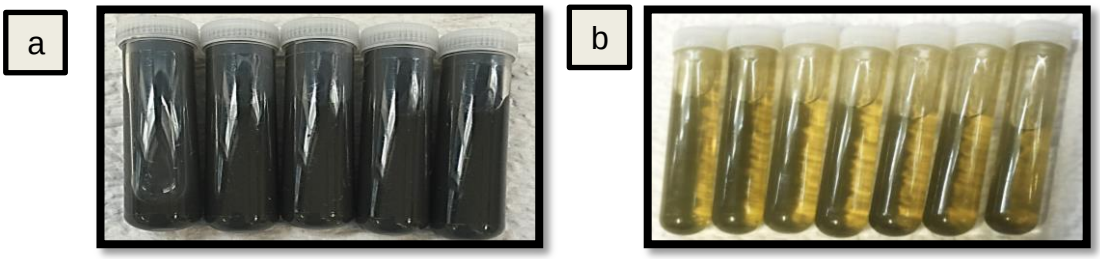

Figure (12): a) MoS_2 dark suspension after sonication, b) MoS_2 yellow suspension after centrifugations.

The thin film was fabricated using vacuum filtration with two types of membranes: mixed cellulose ester membrane (MCE) first one with small nano-sized pores (TYPE VSWP 0.025µm, Millipore "stencil") and over it another one with large nano-sized pores that had four holes (TYPE HAWP 0.45µm, Millipore "target") as shown in Figure (13). Next, the required volume of the suspension was diluted with 250mL of deionised water, filtered with the two membranes, which had differences in the flow rates (between the target and stencil membranes). Indeed, this produced precise film thicknesses and optical densities by changing the volume of the suspensions used as well as well-defined film shapes with identical characteristics onto the target membrane. The filtered film was washed carefully with (3×50mL deionised water). A circular region (0.32cm^2) of the membrane was transferred onto a glass substrate (2×2cm^2) for the transparency and conductivity tests in Figure (15) or onto a silicon substrate (1×1cm^2) and used in MoS_2 characterisations such as AFM, SEM and Raman as shown in Figure (17) as well as onto silicon substrate for solar cell fabrication (1×1.5cm^2) in Figure (20) and this will be repeated for the SWCNTs films and the hybrid MoS_2/SWCNTs.[22]

Figure (13): Mixed cellulose ester (MCE) with four holes to make the electrode.

SWCNTs suspension preparation

0.5mL of Triton X-100 (ALDRICH) was mixed with 49.5mL of deionised water using the ratio (50mL,1%v/v). The suspension was bath sonicated for 20minutes at 50W_{RMS} at the room temperature. After that, 0.005g of large diameter arc-discharged, P3-SWCNTs (Carbon Solution, Inc.) were added then bath sonicated for 1hour. The next step was centrifugation for 1hour at 17500g. The supernatant was collected, recentrifuged for additional 1hour at 17500g. Finally, the supernatant was collected. The colour was black as shown in Figure (14).

Figure (14): CNTs suspension after centrifugation.

Hybrid MoS_2 with SWCNTs

Molybdenum disulfide was hybridised with the carbon nanotubes and attached onto the n-Si solar cell using the vacuum filtration process as mentioned before using various ratio (volumes) of the two stock suspensions after bath sonication for around 10minutes at the room temperature. Moreover, keeping the SWCNTs at the same volume (300μL) and changing the MoS_2 volume (100, 200, 300, 400, 500, 600, 700, 800, 900, 1000μL and 2mL) with 250mL of deionised water. This allowed the production of homogeneous of MoS_2 and SWCNTs aqueous dispersions utilised to make films (electrodes) for device fabrication and other characterisation.

Preparing glass samples for the Conductivity and Transparency analysis

A glass substrate was rinsed with acetone, ethanol and dried with N_2. MoS_2 or SWCNTs films were filtered by the proposed volumes via the vacuum filtration method as mentioned earlier with the same membranes (TYPE VSWP 0.025μm and TYPE HAWP 0.45μm). The film was deposited onto a glass piece ($2\times2cm^2$) centered over the active area following the sandwich procedure. The film was wetted with deionised water and compressed. The first layer is a glass substrate ($2\times2cm^2$) with film deposited over it, a second layer of piece of Teflon. Lastly, after a third layer of glass substrate ($2\times2cm^2$) the substrates are clamped using clips. Subsequently, oven dried at 80℃, for 15minutes, cooled down at the room temperature for 1hour. Later, the glass substrate was immersed in acetone for 30minutes to dissolve the membrane. The glass sample rinsed with fresh acetone, stirred for 30minutes and N_2 dried. The resulting sample is a glass substrate with the film ($0.32cm^2$) deposited over it as shown in Figures (15) and (16). The glass treatments were 2%HCl instead of 2%HF because it dissolves the glass thus one drop of the 2%HCl over the film's surface for 15seconds, next, rinsed with deionised water, ethanol and dried with N_2. The second treatment was the thionyl chloride $SOCl_2$, one or two drops over the active area, left to dry in air, rinsed with ethanol and dried with N_2. The third treatment was again the 2%HCl. Afterward, the sample was ready for Conductivity (Sheet resistance) and Transparency (Optical characterisations) analyses (see Figures (15) and (16)).

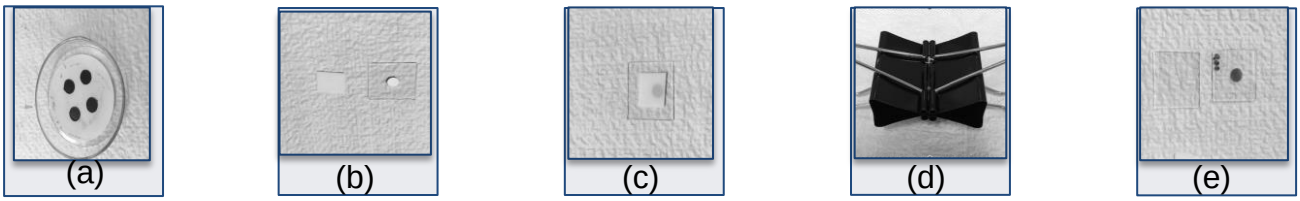

Figure (15): The film attachments' on a glass substrate process, (a Cut the active area (0.32cm^2), b) Place the film (electrode) upside down and wet with drop of deionised water, (c Place the Teflon piece over the film, (d Clamp the glass substrates with the clips, (e After oven dry, cool down, then dissolve the membrane by acetone and the sample was ready for measurements.

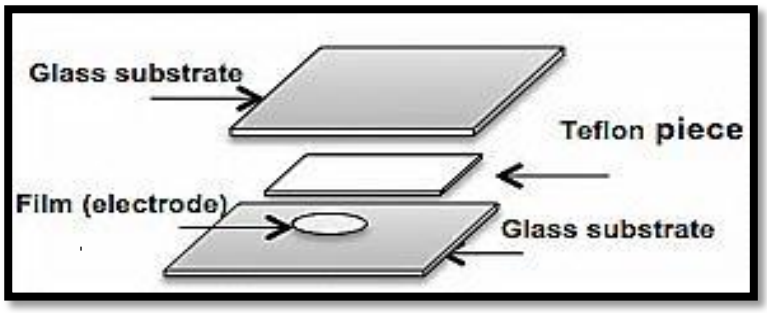

Figure (16): A schematic of applying the electrode over a glass substrate for both the conductivity and transparency analysis.

Cleaning the Silicon wafer for the AFM, SEM and Raman analysis

Silicon substrates were cleaned by bath sonication at the room temperature in acetone for 10minutes (rinsed with deionised water, ethanol and dried with N_2). Again using the same manner as mentioned in the previous section but the electrode (film) deposited over a silicon substrate (1×1cm^2) not glass. The sample was a silicon substrate with the film (0.32cm^2) deposited over it. The sample was ready for SEM; AFM and Raman characterisation (see Figures (17) and (18)).

Figure (17): a) 1×1cm^2 silicon piece placed over 2×2cm^2 glass substrate. b) The film deposited facing down over the Si substrate. c) A piece of Teflon placed on top of the film. d) Another glass substrate applied on top of the Teflon. e) The layers clamped together using clips.

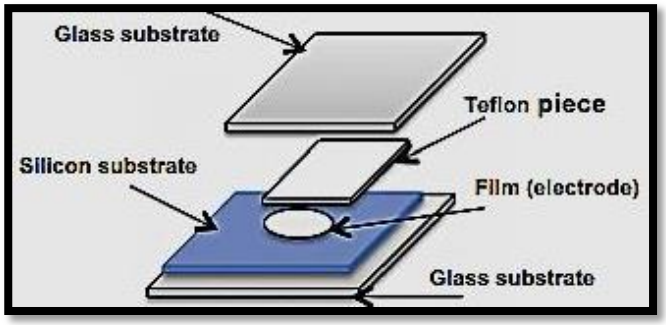

Figure (18): A schematic of applying the electrode over the silicon substrate for AFM, SEM and Raman analysis.

Characterisation of Single Wall Carbon Nanotubes, Molybdenum Disulfide and Hybrid Molybdenum Disulfide with Single Wall Carbon Nanotubes

Atomic Force Microscopy (AFM)

The MoS_2, SWCNTs and hybrid MoS_2/SWCNTs films made with different suspension volumes were mounted on silicon substrates and examined (height measurements) using both Multimode Nanoscope AFM V and V 2 (tapping mode) with different parameters setting such as, sample/line (512), set point (300-700mV), scan rate (1-2Hz), scan size (1-5μm), driving amplitude (~100mV), and integral gain (3-4).

Scanning Electron Microscopy (SEM) (Inspect FEI F50 SEM)

The MoS_2, SWCNTs and hybrid MoS_2/SWCNTs films with different ratio filtrations were deposited on silicon substrates and observed using Inspect FEI F50 SEM with different parameters setting such as, acceleration voltage (10-20KV), spot size aperture (4), working distance (9-10mm).

Raman Spectroscopy (Horiba Xplora Raman)

The MoS_2, SWCNTs and hybrid MoS_2/SWCNTs electrodes with different volume filtrations were placed on silicon substrates, and analysed using (Horiba Xplora Raman) with different parameters setting such as excitation wavelength (532nm), microscope objective (10x and100x), acquisition time (1-5seconds).

Preparing the SWCNTs-n-Silicon and Hybrid MoS_2/SWCNTs-n-Silicon Solar Cells

There were many steps to prepare the solar cells and each solar cell was prepared several times and average measurements were obtained.

Silicon wafer Preparation

Cleaning the silicon n-type substrate (CZ, 5-25Ω.cm, <100>mm diameter single- SSP, ABC GmbH with thermal oxide with 100-nm side polished, thickness 525±25μm, n/phosphorous-doped and SiOx layer, München) was done as follows: Piranha mixture was prepared from hydrogen peroxide (H_2O_2, 10mL) and sulfuric acid 30% (H_2SO_4, 15mL) inside the fume hood in cylinder up to 25mL. Next, the silicon wafer was put in a large circular plastic petri dish, the piranha mixture added and covered for 10minutes. After that the silicon was rinsed with deionised water, then bath sonicated in acetone for 10minutes and dried with N_2. The silicon wafer was ready for the mask process (photolithography). Disposing of the waste of the piranha mixture was done by putting the solution into a beaker, the pH tested and if it too acidic made it neutral by adding sodium hydroxide (solid) or potassium hydroxide (liquid). After dissolving, test the pH again until less than 4; finally, under running water the solution was discarded.

Applying the mask onto Silicon wafer (Photolithography)

The stages of applying the mask pattern to the silicon wafer are shown in Figure (19).

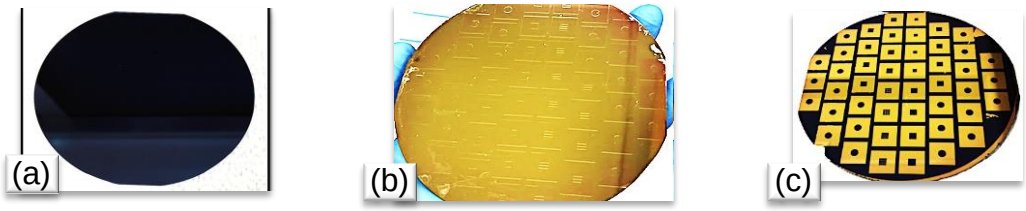

Figure (19): The photolithography attachment onto silicon substrate.

This was done after the silicon wafer was cleaned (see Figure (19 a)). Then a thin layer of the photoresist (AZ 1518) was placed the silicon and spun on the spin coater for 30seconds. This was to help spread the positive photoresist over the top of the silicon wafer. The photoresist was dried by heating on the hot plate (100degree) for 1minute, cooled down at the room temperature. Later, UV light shone through a mask (photolithography) for 30seconds printed the mask pattern over the silicon substrate see (Figure (19 b)). The substrate was then inserted into the developer solution (AZ 326 MIF) for 1minute and lastly, rinsed with distilled water and dried with N_2. Following that the silicon wafer was coated with gold and chromium using the sputter coater. After, coated the silicon substrate immersed in acetone for 30minutes and stirred slightly. The silicon wafer appeared as rectangular metals coated with circular regions ($0.08cm^2$). These regions will be without metal coated after dissolving in acetone bath as shown in Figure (19 c). The silicon substrate was ready for the buffered oxide etching (BOE) in order to remove the oxidised layer from the active region.

Buffered Oxide Etching (BOE) Treatment

BOE (buffered oxide etching) treatment was done by applying one drop of (BOE) over the circular active area with a diameter of ($0.08cm^2$) for around 2minutes. The silicon substrate was then rinsed with (deionised water, ethanol) and dried with N_2. The film (SWCNTs or MoS_2-MCE membrane, $0.32cm^2$) was deposited onto the silicon substrate with the film side down centred over the active area (etched hole). The film was wetted with one drop of deionised water and compressed using the sandwich method. This method is a glass layer over it silicon substrate that had the film deposited on it, covered by a piece of Teflon. Finally, a glass layer then clamped using clips as shown in Figure (20). The sample was then baked dry (80℃, 13minutes followed by cooling down at the room temperature for 5hours). Subsequently, the membrane (MCE) dissolved by immersing the silicon substrate in acetone for 30minutes. The device washed with fresh acetone, stirred for 30minutes and N_2 dried. The final device was a silicon substrate with active area ($0.08cm^2$) surrounded by the film ($0.32cm^2$) that overlapped the front metal contact. Etching the cell's rear oxide to make it

conductive allowed contact with gallium-indium eutectic (eGaIn -ALDRICH) at the back that mounted on steel plate ($2\times2cm^2$). The device was prepared for testing the efficiency using the solar simulator at this stage; the device was called as prepared solar cell.

Hydrofluoric Acid (%2 HF) Treatments

The first treatment was a 2% HF (Hydrofluoric acid) treatment made by dropping one drop of 2% HF over the active area for 15seconds followed by a rinse with water, ethanol and dried with N_2.The purpose of this was to remove the oxide layer from the silicon. The second treatment was a thionyl chloride ($SOCl_2$) treatment completed by applying one drop over the film in order to make the CNTs more conductive. The sample was left in air to dry, and then rinsed with ethanol and N_2 to dry. The third treatment was the 2% HF again by the same manner to remove the oxidisation from the thionyl chloride step. After each treatment the efficiency was tested and after the final treatment as well for the final efficiency. Finally, the MoS_2/CNTs film will be deposited onto the n-Si based solar cell using the same procedure (see Figures (20) and (21)) and the efficiency tested and compared for both solar cells.

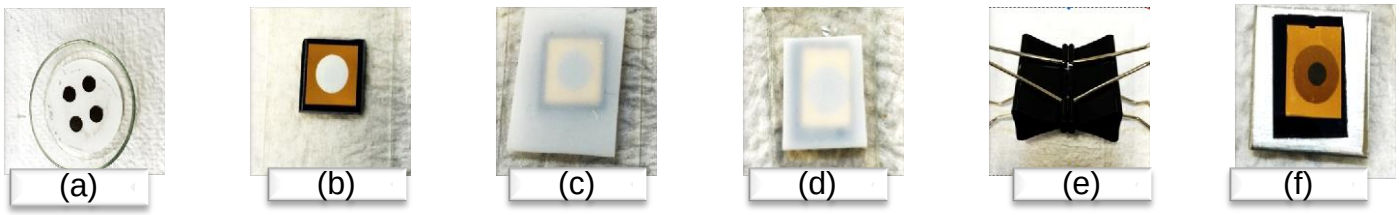

Figure (20): The solar cells preparation steps, (a Cutting the film (active area, $0.32cm^2$), (b Attaching the film upside down the silicon substrate and wetting with drop of water, (c Covering the cell with a piece of Teflon, (d Placing glass substrate over the Teflon piece, (e Clamping the substrates using clips and drying for 13minutes then cooling down for 5hours, (f Dissolving the membrane using acetone and etching the rare back of the silicon, putting a little of indium gallium and applying a piece of steel, the device was ready for treatments and testing.

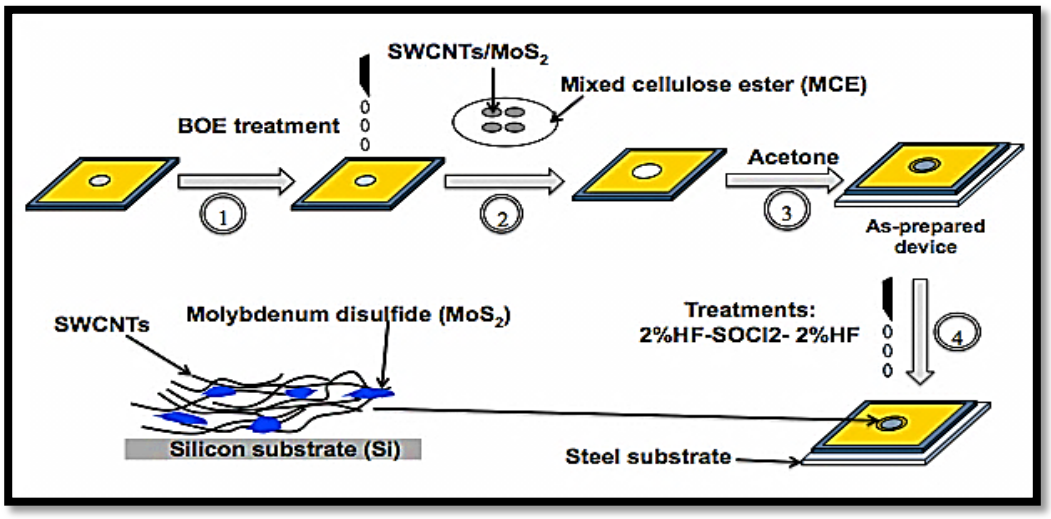

Figure (21): A schematic of the solar cell device fabrication.

Characterisation of SWCNTs-n-Silicon and Hybrid MoS_2 /SWCNTs-n-Silicon Solar Cells

Solar Simulator (J-V curve) (Efficiency measurements)

The efficiency of the solar cells was examined using the solar simulator, software (Labview), and current data was measured using the (Keithley 2400 source). There were some parameters in this device (solar cells) to observe; for instance: J_{sc} : is the short circuit current density: maximum current when the voltage across the device is zero. V_{oc}: is the open circuit voltage: maximum voltage occurs when the current through the device is zero. FF: is the fill factor: determined from the maximum power from a solar cell. PCE : is the efficiency: the ratio between the output from the solar cell to the input from the light. R_{series}: is the series resistance and R_{shunt}: is the shunt resistance (see Figure (22)) an example for a typical J-V curve and the solar cells' parameters.[1,27] Two types of measurements, the dark current and the light current were taken which provided the efficiency.

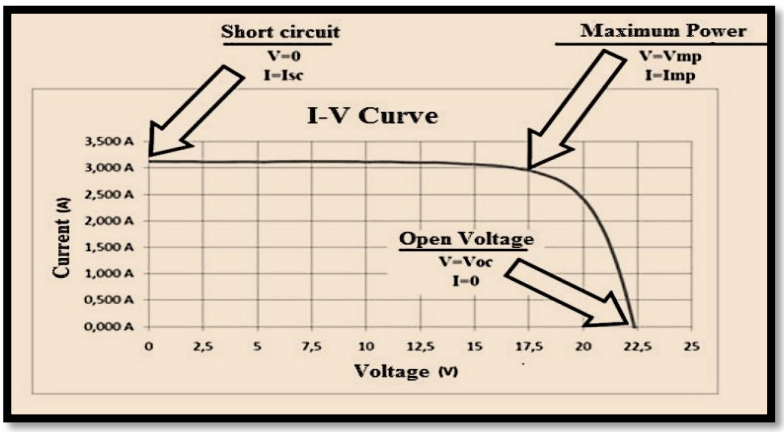

Figure (22): A typical J-V curve with the solar cell parameters. [28]

The Four-Point Probe (Conductivity measurements)

The conductivity test was done using the four-point probe (KeithLink), an average of three readings were taking by measuring (the sheet resistance and conductivity) for the film mounted on a glass substrate by changing the orientation of the glass substrate.

UV-Visible NIR Spectroscopy (Transmittance measurements)

The MoS_2/SWCNTs films on glass substrates were scanned over (UV visible spectrophotometer Cary50, Varian) 350nm to 1000nm in order to test the films' transparency. At the beginning of the test a clean glass slide was used as a blank sample (background). The transparency was calculated from the transparency data using the average at 450nm and 850nm or just at 550nm using the equation.

$$\%\,T = \%T_{550} = \frac{\%T_{450} - \%\,T_{850}}{2}$$

$$\%\,T = \ 10^{(2-Abs.)}\ ^{1}$$

Chapter 3: Results and Discussions

Characterisation of Molybdenum Disulfide, Single Wall Carbon Nanotubes and Hybrid Molybdenum Disulfide with Single Wall Carbon Nanotubes.

Atomic Force Microscopy (AFM)

AFM images of MoS_2

AFM scans were used to prove the presence of the chemically exfoliated MoS_2 flakes. From Figure (23 a): AFM image (2.4×2.4µm) for the MoS_2 using filtration volume of (300µm), which displays a large MoS_2 flake.

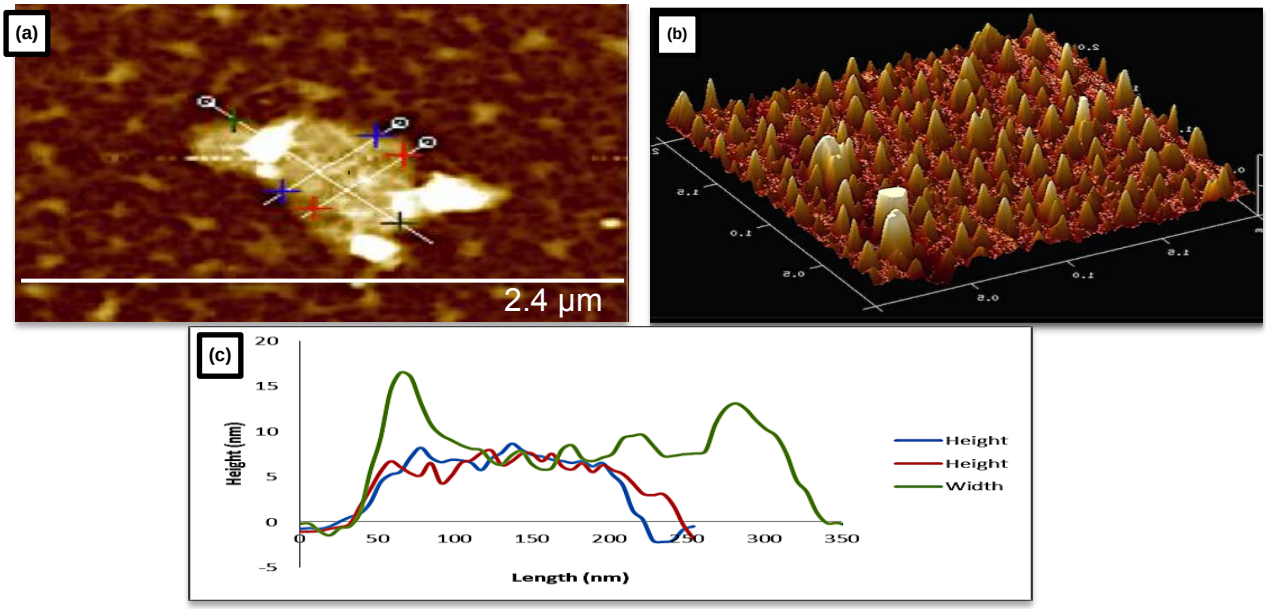

Figure (23): a) AFM images of the height for MoS_2, b) 3D image for the same sample, c) The MoS_2 flake's height and width for figure (a).

Figure (23 b) shows a topographic image that had many small molybdenum flakes, which created rough surface, and this is vital in order to reduce the light reflection thus, improving the solar cell charge carrier separations and overall cell's performance. [29] Figure (23 c): illustrates the thickness of the MoS_2 large flake (a few hundred nanometers in lateral dimensions) that in the Figure (23 a) which was ~5nm thick because there were a number of layers on top of each other. From literature [22,30] the average thickness for monolayers was ~1.3nm and the lateral size for the exfoliated layers was around 300nm. From this sample's results, which agreed with literature, it was clear that the exfoliation of MoS_2 crystals were successfully achieved.

AFM images of SWCNTs

An AFM image (3×3µm) for the SWCNTs bundles with volume filtration of (300µL) deposited on Si substrate was scanned to prove there was some CNTs to be able to hybridised with MoS_2 and the image collected is shown in Figure (24 a) and its 3D image in Figure (24 b).

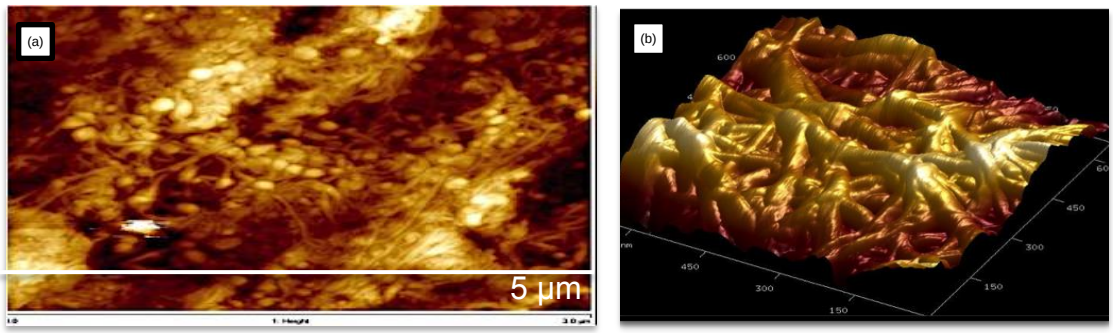

Figure (24): a) AFM image of the SWCNTs, b) 3D image for the same sample.

AFM images of Hybrid MoS_2 with SWCNTs

Here atomic force microscopy was used to display how MoS_2 and SWCNTs hybridise. The AFM image (5×5µm) in Figure (25 a) is for the MoS_2/SWCNTs film with filtration volume (600µL) of MoS_2 with a control volume (300µL) of SWCNTs placed on silicon substrate. Figure (25 b) shows the topographic image for the hybrid MoS_2 with SWCNTs.

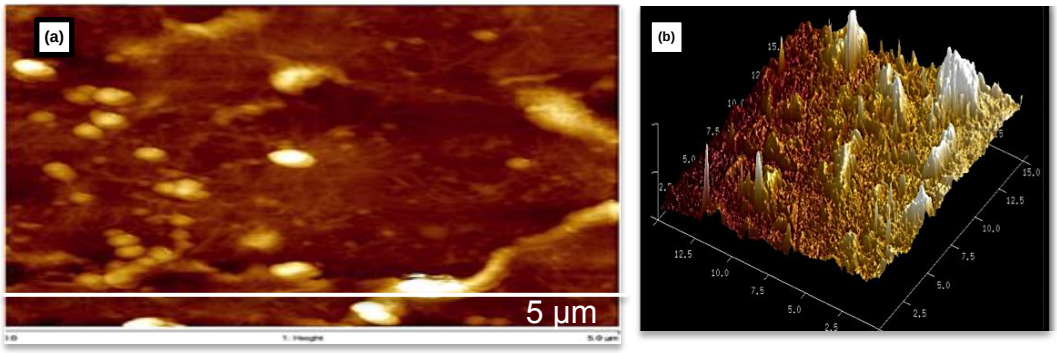

Figure (25): a) AFM image for the hybrid MoS_2/SWCNTs, b) 3D image for the same sample.

Scanning Electron Microscopy (SEM) (Inspect FEI F50 SEM)

SEM images of MoS_2

SEM images were taken in order to investigate the presence of molybdenum disulfide flakes with filtration volume of (1mL). Figure (26a) shows MoS_2 flakes that involved a number of layers set on top of each other. Herein, the EDX spectrum observed in Figure (26 b) proved the existence of MoS_2 peaks and the silicon peak as the background substrate where the MoS_2 was mounted. In Figure (26): the MoS_2 flakes had a lateral size of (~500nm-1µm).

(a) (b)

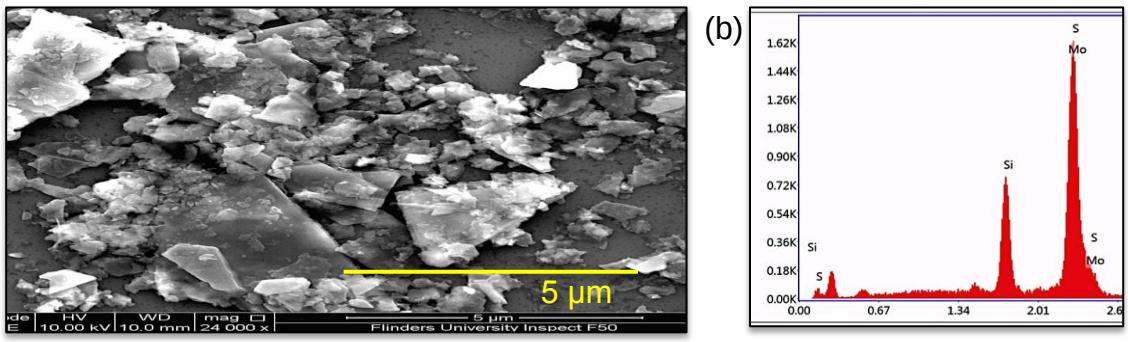

Figure (26): a) SEM image for the MoS_2 flakes. b) The EDX spectrum for the MoS_2 flakes.

SEM images of SWCNTs

Figure (27 a) depicts the SEM image (2×2µm) of SWCNTs (150µL) that were randomly aligned on the silicon substrate (spider web) and Figure (27 b) displays the EDX spectrum that shows the presence of carbon as well as the silicon peak as the background.

(a) (b)

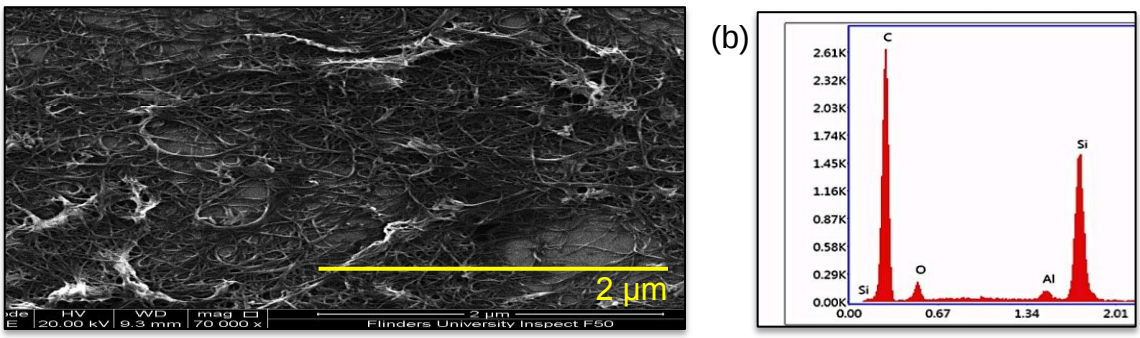

Figure (27): a) SEM image for the SWCNTs. b) The EDX spectrum for the SWCNTs.

SEM images of Hybrid MoS_2 and SWCNTs

Figure (28 a) shows the SEM image (40×40µm) for the hybrid MoS_2 (300µL) and SWCNTs (300µL). The MoS_2 flakes were the white small sheets surrounded by the SWCNTs and some of them cover with the SWCNTs. Figure (28 b) is the EDX, which shows the presence of molybdenum, sulfur and carbon, the silicon peak as the background substrate.

(a) (b)

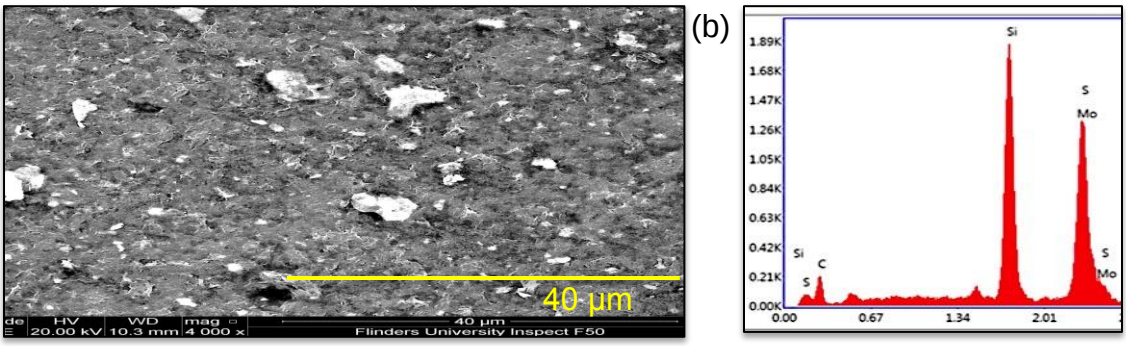

Figure (28): a) SEM image for the hybrid MoS_2/SWCNTs. b) The EDX spectrum for the hybrid MoS_2/SWCNTs.

(a) (b)

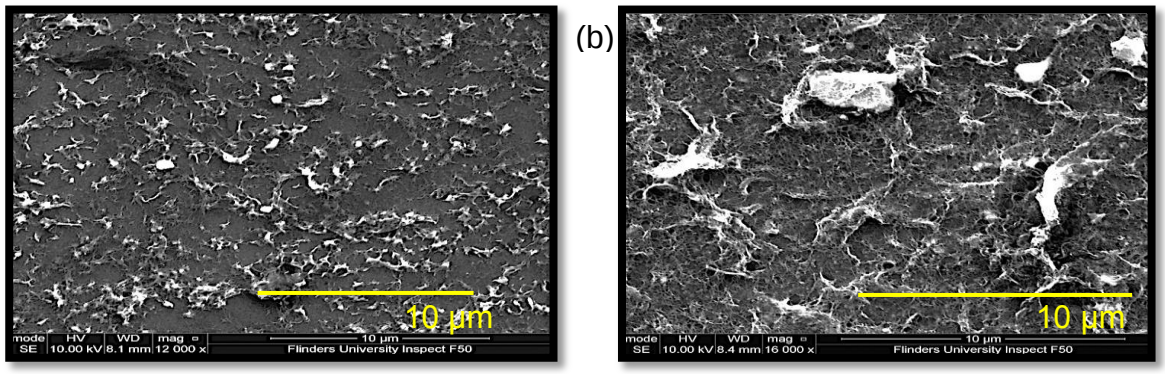

Figure (29): SEM images that show the different between MoS_2/SWCNTs films thickness, a) Film with filtration thickness of (200µL MoS_2/150µL SWCNTs) in contrast b) Film with filtration thickness of (1200µL MoS_2/900µL SWCNTs).

From Figures (29 a, and b), there was a comparison between the two samples of hybrid MoS_2/SWCNTs with the same ratio of volumes (3:4) but different film thickness. Figure (29 a) (200μL MoS_2/150μL SWCNTs) exhibits some empty areas through to the silicon background substrate whereas in Figure (29 b) (1200μL MoS_2/ 900μL SWCNTs) a more complete coverage was observed. This indeed, reflected the quality of the solar cells where in the first case the CNTs create the depletion region with the n-silicon semiconductor since, the CNTs can reach the Si substrate. In the second case the materials limited the CNTs in direct contact with the silicon substrate because the MoS_2 film is thicker in this situation whereas, the first case, the MoS_2 film is really thin. As a result, in the first case, the depletion region was created between the CNTs and the silicon substrate while; in the second case the depletion region created between the SWCNTs (p-type semiconductor) and the MoS_2 (n-type semiconductor). This produced different cell performance as the film thickness affected the transmittance and conductivity of the cells.

Raman Spectroscopy (Horiba Xplora Raman)

Raman spectrum for MoS_2

In order to ensure the existence of molybdenum disulfide, Raman spectra were obtained. Raman can indicate how many layers of MoS_2 were present. The Raman spectrum for the chemically exfoliated MoS_2 shows two noticeable peaks due to vibrations the in-plane E^1_{2g} vibration. Furthermore, (the molybdenum and sulfur vibrate in plane direction) and the out-of-plane vibration A_{1g} (the sulfur vibrates perpendicular- to-plane direction).[22,29] In fact as shown in Figure (30), there were further weak peaks that occur at lower frequencies, which correspond to the J_1, J_2, and J_3 modes that were allowed in 1T- type MoS_2 (metallic phase) and not allowed in 2H-MoS_2 (semiconducting phase). MoS_2 characteristic Raman peaks appeared at ~385 and ~405cm^{-1} (the MoS_2 peaks were not strong perhaps because the acquisition time was very fast (1-5seconds) or the scanned spot did not have enough material) which signify E^1_{2g}, and A_{1g} vibrations modes respectively for this sample which were similar to those reported in the literature (see Figure (31)).[22,29] Where ~520cm^{-1} corresponds to the silicon peak (the Si peak was small because the film was really thick (1mL of MoS_2) and this can limit the light reaching the Si substrate) from the background substrate sample.

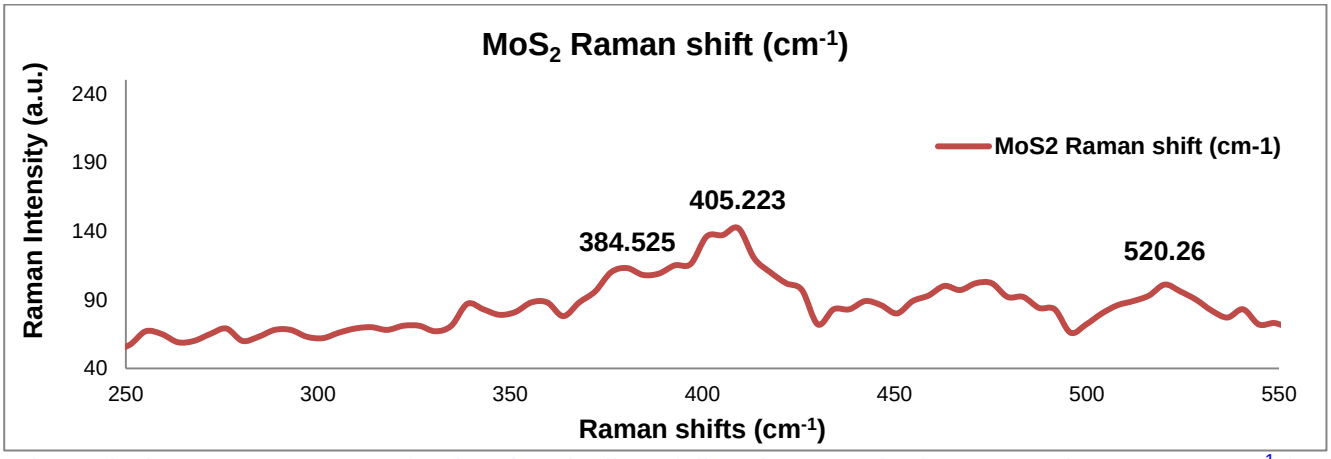

Figure (30): Raman spectrum for the chemically exfoliated MoS_2. The largest peaks are ~385cm^{-1} for E^1_{2g} and ~405cm^{-1} for A_{1g} both for MoS_2 and ~520cm^{-1} for Silicon.

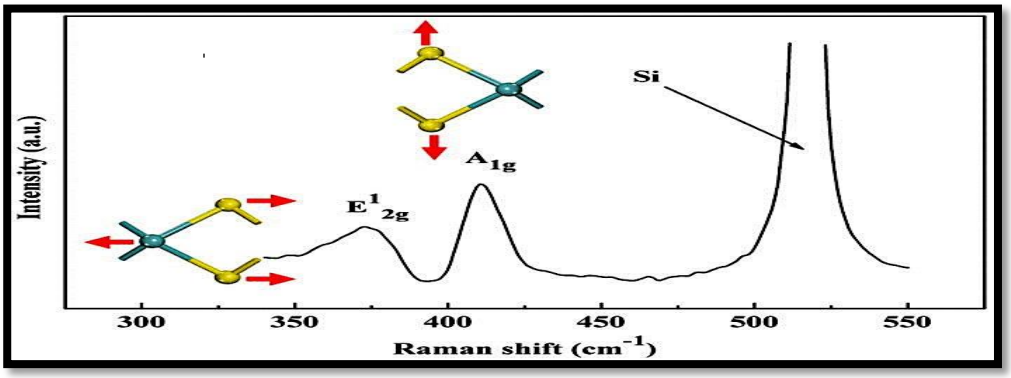

Figure (31): Raman shift for the MoS_2 with its vibrations modes $E^1_{2g}$and A_{1g}.[29]

The E^1_{2g}, and A_{1g} peak positions depend on the number of layers or layer thickness, as a result in this sample it was for monolayers because the peak separation between peak $E^1_{2g}$and A_{1g} peak was 20cm^{-1}. From literature, for bulk and monolayers of molybdenum disulfide the frequencies differences between $E^1_{2g}$and A_{1g} peaks were 25 and 19cm^{-1} respectively.[19,31] Additionally, as Jariwala et al. reported the separation between the peaks $E^1_{2g}$and A_{1g} was considered a perfect parameter to determine the thickness for ultrathin molybdenum disulfide. Accordingly, when the parameter Δ had a value of 20cm^{-1} or less between the E^1_{2g} and A_{1g} modes that indicated the presence of single layers of MoS_2. In contrast, when the Δ value was over 20cm^{-1} that implied multilayers of MoS_2. In this case, this MoS_2 sample showed that the separation between the two peaks is 20cm^{-1}and that means this sample few layer.[32-34]

Raman spectrum for SWCNTs

From the Raman spectrum in Figure (32), the characteristic peaks of SWCNTs were detected at ~162, 1332, and1586.89cm^{-1} and represent the radial breathing modes (RBMs) at low frequencies, D-band, and G-band at high frequencies respectively. Whilst, the silicon

peak occurred at 520cm^{-1} (the same situation with the Si peak the CNTs film was thick 1mL and this was why the peak small). Figure (33) from literature shows their results matched with this SWCNTs sample.[35,36]

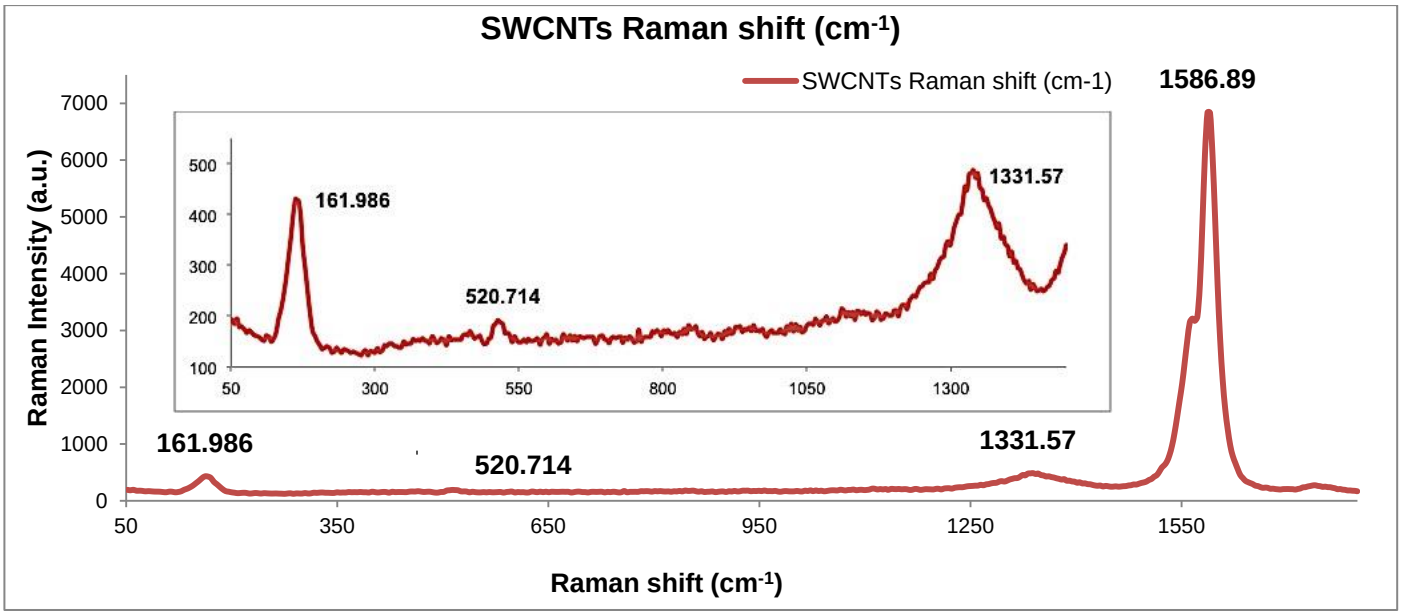

Figure (32): Raman spectrum for the SWCNTs. The largest peaks were for ~162, 1332, and1587 cm^{-1} for SWCNTs and ~520cm^{-1} for Silicon.

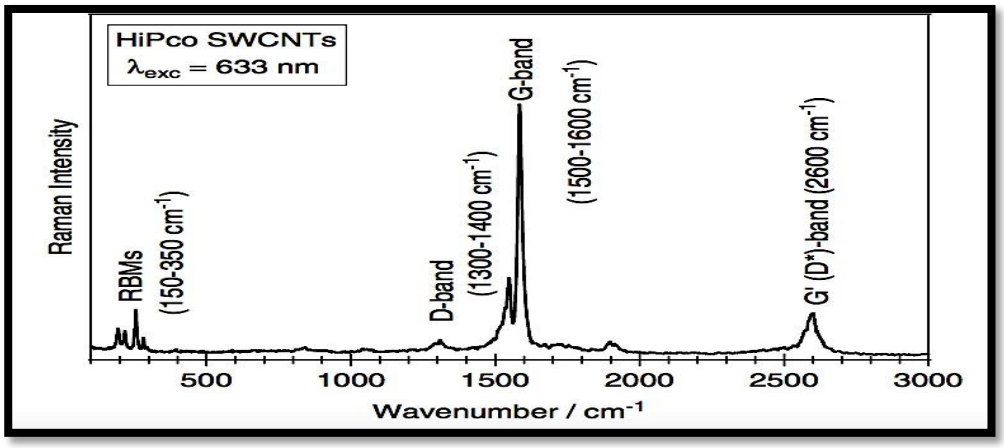

Figure (33): Raman spectrum for the bulk SWCNTs.[35]

Raman spectrum for Hybrid MoS_2 and SWCNTs

The MoS_2/SWCNTs films with (300µL) of MoS_2 and (600µL) of SWCNTs mounted on silicon substrate were tested and this was the third technique that used to show hybridisation was achieved and then these samples can be implemented in the solar cells. Figure (34) shows the Raman spectrum for both hybrid MoS_2 with SWCNTs that revealed the characteristic peaks as followed, ~386 and ~404cm^{-1} for MoS_2 as they represented E^1_{2g} and A_{1g} peaks respectively (these peaks were not strong because the filtration amount of the MoS_2 was less compared to CNTs).[31,35]

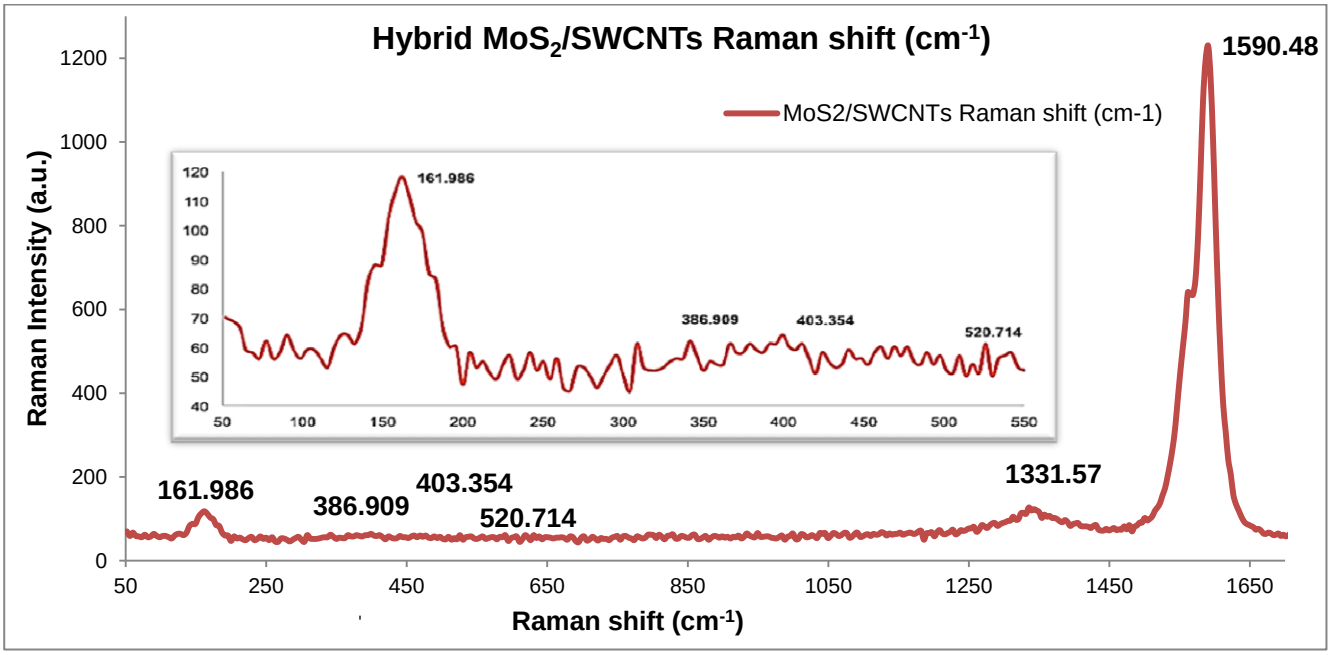

Figure (34): Raman spectra for the hybrid chemically exfoliated MoS_2 and SWCNTs. The largest peaks were for ~387, ~404cm^{-1} for MoS_2 and ~162, ~1332 and ~1591cm^{-1} for SWCNTs and peak ~520cm^{-1} for silicon.

Characterisation of SWCNTs-n-Silicon and Hybrid MoS_2 /SWCNTs-n-Silicon Solar Cells

Single Wall Carbon Nanotubes- Silicon based Solar Cells experiment.

In order to understand the effect of molybdenum disulfide on the CNTs-n-type monocrystalline silicon based solar cells the first step was to prepare the CNTs-n-Si based solar cells and make a comparison between the CNTs-Si based and MoS_2/CNTs solar cells to get an answer about the difference in terms of efficiency. The depletion region here is created between the p-type SWCNTs and the n-type silicon substrate as shown in Figure (9). There are many factors that influence the cell performance; for instance, the transmittance and this is how much light gets through the electrode, which is determined by the film thickness. Another factor is the sheet resistivity and this is the resistivity of the electrode. Reducing the film thickness raises the transparency of the film but decreases the sheet resistivity (high conductivity) will increase the device's efficiency. In short, both the transparency and sheet resistivity are pivotal factors that rise the cell's electricity generation.[1] The CNTs-Si based solar cells were fabricated as explained in the experimental section based on the literature.[1] After preparing the CNT suspension and fabricating the devices, the UV-visible spectrum was obtained to measure the transparency. The results were shown in Figure (35) giving a transparency of ~73% and considered an optimal value as stated in literature[1], along with low value for the sheet resistivity with an average reading 192$(\Omega \, . \, \mathrm{cm}^{-1})$ (see Table (A1) in the Appendix). For further experimental details see Tables (A1) and (A2) in the Appendix, Tables (1) and (2) demonstrate the average parameters for three cells with the same suspension volumes of CNTs (300μL).

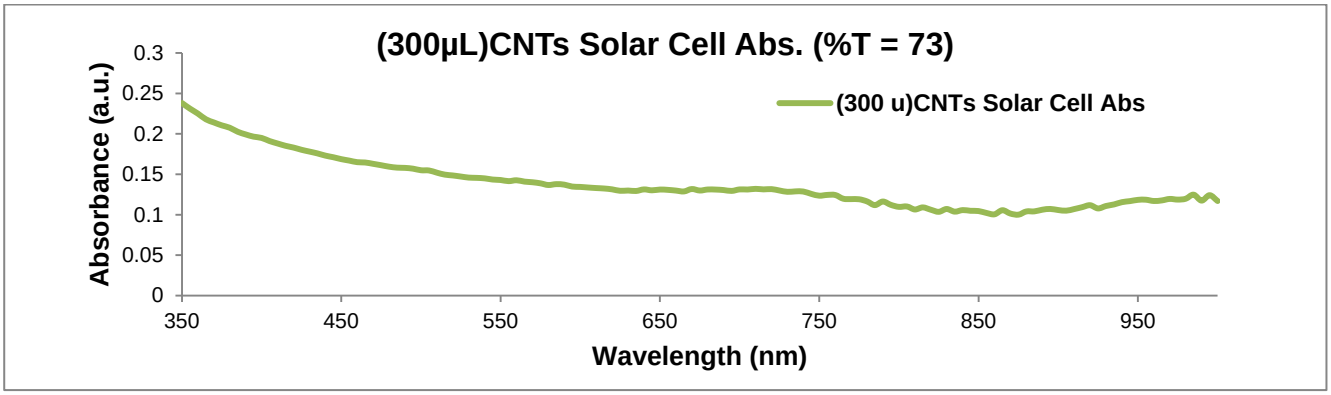

Figure (35): The absorption spectrum for the pristine (300µL) SWCNTs-n-silicon solar cell (2).

Table (1): The pristine SWCNTs-n-Si solar cells with controlled volume of SWCNTs (300µL) and their parameters (Transmittance (T %), Sheet Resistivity($\Omega.\,cm^{-1}$), and Efficiency (%E)).

Cell Name	Transmittance (T %)	Sheet Resistivity ($\Omega.\,cm^{-1}$)	Cell Efficiency (%E)	Highest, Average Cell Efficiency (%E)
300µL SWCNTs (1)	73.4	192	6	7.5, 7 ± 0.63
300µL SWCNTs (2)	73.2	188.3	7	
300µL SWCNTs (3)	72	187	7.5	

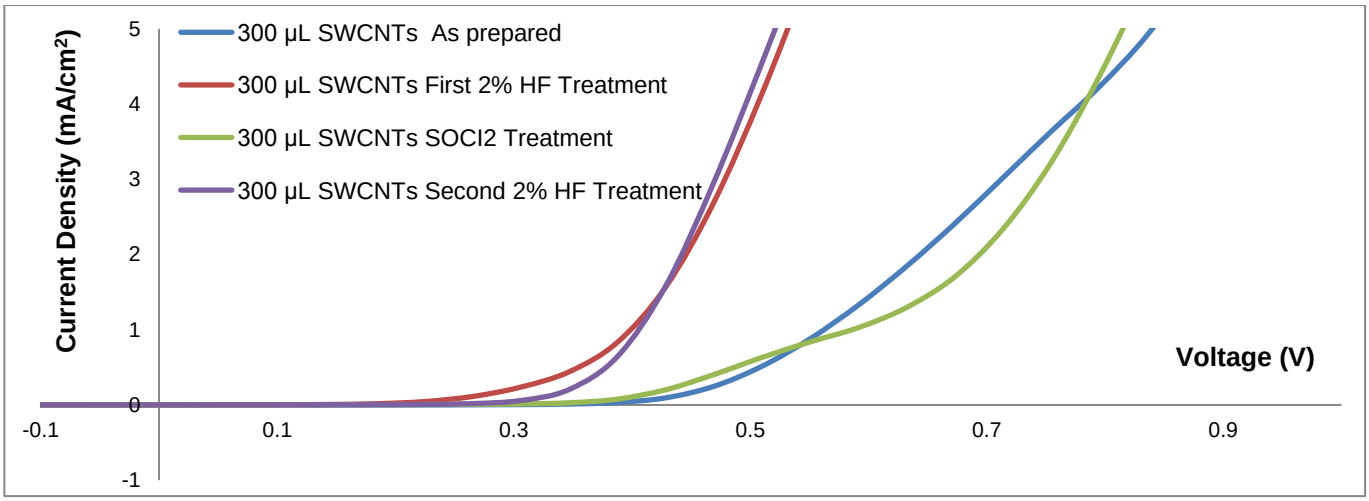

Figure (36): Dark curves for the SWCNTs-n-Silicon based solar cell, SWCNTs (300 µL) cell (2).

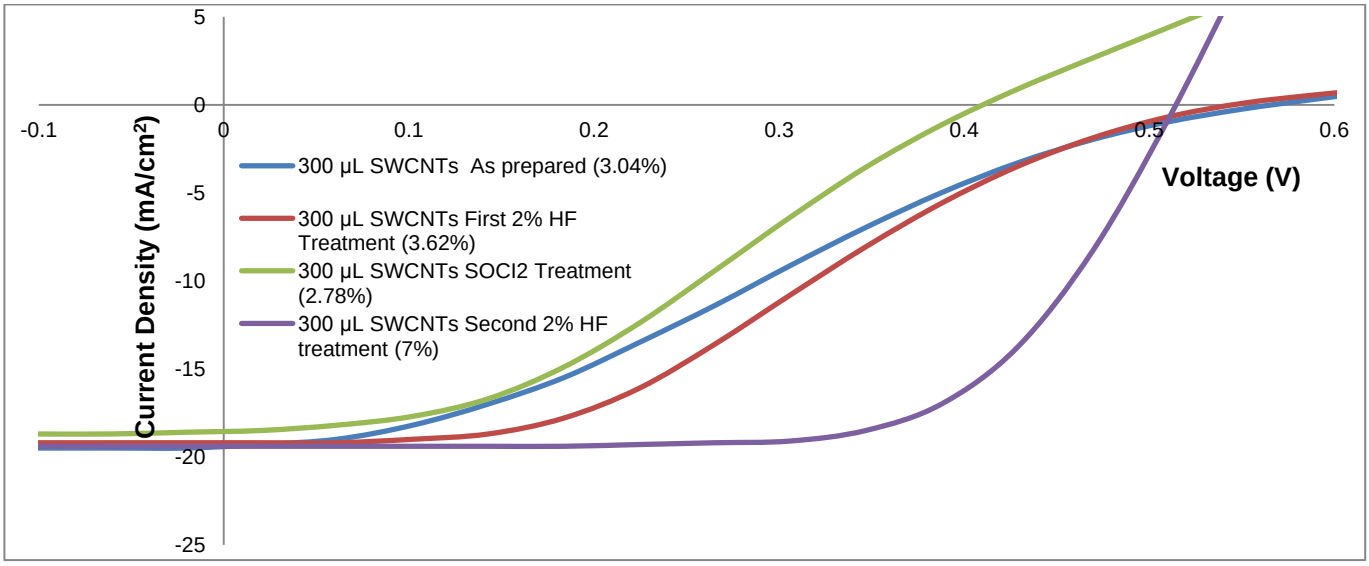

Figure (37): Light curves for the SWCNTs-n- Silicon based solar cell, SWCNTs (300µL) cell (2).

Table (2): The parameters of the best efficiency for the pristine SWCNTs-n-Si solar cells (Short circuit current J_{sc} (mA/cm^2), Open circuit voltage V_{oc}(V), Fill Factors (FF), Efficiency (%), Current shunt resistance R_{shunt} (Ohms), and Series resistance R_{series} (Ohms).

Cell Name	J_{sc} (mA/cm^2)	V_{oc} (V)	FF	R_{shunt} (Ohms)	R_{series} (Ohms)
300 µL SWCNTs (1)	22.029	0.501	0.53	4.81E+03	7.53E+01
300 µL SWCNTs (2)	19.387	0.515	0.66	6.75E+04	6.92E+01
300 µL SWCNTs (3)	24.114	0.515	0.6	5.29E+03	1.05E+02

Figures (36) and (37) indicate the performance of the standard SWCNTs-n-silicon solar cell and the effects before (as-prepared cell) and after the three treatments which were the first 2% HF etching, the thionyl chloride ($SOCl_2$) and the second 2% HF etching. Before applying the film (SWCNTs electrode) BOE was used to remove the oxide layer from the silicon substrate (the active area), which improved the final efficiency of the device. The efficiency for the as- prepared cell was tested using both dark and light current-voltages characteristics before and after each treatment (Figures (36) and (37)). The as-prepared CNTs-Si solar cell as illustrated in Figure (20) gave an efficiency of 3.04%, and after first treatment was 3.62%, after the second treatment was 2.78%, and finally, after the third treatment was 7%. Moreover, for the first 2% HF treatment (15seconds), the efficiency increased compared to the as prepared cell (post-treatments) because of the 2% HF effect in removing the oxide layer between the SWCNTs film and the silicon substrate. The oxide layer insulation and stop the development of the depletion region.[1,37] The second treatment, one drop of the thionyl chloride (chemical doping of $SOCl_2$) was applied. The efficiency dropped because the role of the organic oxidizer ($SOCl_2$) is to increase the SWCNTs conductivity, minimise the sheet resistivity also, where the $SOCl_2$ function is to prevent the CNTs from the tunnelling behaviour by adjusting the SWCNTs' Fermi level. Still, as the thionyl chloride interacted with the silicon substrate and forms an oxide layer the cell efficiency fell from 3.62 to 2.78%.[1,38,39] The third treatment, the second 2% HF etching removed the oxide layer that forms after the thionyl chloride treatment. Indeed, this treatment lifted the cell's PCE from 2.78% to 7% along with the short circuit current J_{sc} from 18.556 to 19.387(mA/cm^2), the open circuit voltage $V_{oc}$from 0.411to 0.515V, the fill factor (FF) from 0.28 to 0.66, the R_{shunt} (Ohms) from 2.42E+03 to 6.75E+04Ω, and the R_{series} (Ohms) from 7.00E+02 to 6.92E+01Ω. Overall, the HF treatments enhanced the cell efficiency and the fill factor for thinner films despite the fact that after 1hour within the lab environment, the efficiency dropped to 5% because the oxide layer (SiOx) started to form again and after 1week the efficiency went back to the as prepared cell~3%. Hence, there was a remarkable increase after the previous treatments in the efficiency from ~3% to 7% as well as the other parameters.

Electrochemical Etching (2%HF) experiment

In this experiment, as mentioned before the treatments are essential for the solar cells performance. At the beginning of the project, it was noticed that sometimes the cell required more than 15second of 2% HF etching. Additionally, the efficiency after third 2% HF treatment sometimes increased and others decreased. Consequently, three solar cells were made with the same conditions (same ratio filtrations) of 300µL SWCNTs+400µL MoS_2. Except, the etching time was changed starting with the normal time 15seconds for each one and after getting the final efficiency additional etching time were attempted for each cell. Thus, increased the time to an additional 15seconds for cell (1), 30seconds for cell (2) and 45seconds for cell (3). All the experimental data are in Tables (A3), (A4) and (A5) in the Appendix. The best cells' performance details are in Tables (3) and (4), with their corresponding J-V curves in Figure (38). The results were as follows: all of them have similar transmittance values ~ 65, 65 and 67%, and the sheet resistivity values were 376, 351.2, and 297$(\Omega.\mathrm{cm}^{-1})$ for cells (1), (2) and (3) respectively. The pure CNTs cell had an ideal transmittance 72% with a low sheet resistivity 187$(\Omega.\mathrm{cm}^{-1})$. The short circuit current enhanced with the addition of 2% HF etching from 22.517 to 24.177(mA/cm^2) where the former value was similar to the pristine CNTs cell and the fill factors showed a slight increased for the hybrid MoS_2/SWCNTs. The fill factor for the SWCNTs cell was 0.6 where the average for the hybrid MoS_2 and SWCNTs was 0.63. The efficiencies values were 8, 8 and 8.62% respectively where; the base CNTs was 7.5%. In contrast, after applying the extra etching time for all three cells, there was an obvious reduction in all parameters including, the efficiency which appeared to fall as the 2% HF etching time increased, 7.5, 7 and 6.5%. The J_{sc}, V_{oc} and FF likewise, reduced with additional etching time. In short, the optimised 2% HF etching time was 15 seconds as reported in literature[1], accordingly, this etching time will be followed in this project because it associated with the best cell's efficiency and parameters.

Table (3): The hybrid MoS_2/SWCNTs-n-Si solar cells with, the same volume filtrations of MoS_2 (400µL) and of SWCNTs (300µL) and normal and extra 2% HF etching and their parameters (Transmittance (T%), Sheet Resistivity $(\Omega.\mathrm{cm}^{-1})$, and Efficiency (%E)).

Cell Name	Transmittance (T%)	Sheet Resistivity $(\Omega.\mathrm{cm}^{-1})$	Normal Etching Efficiency(%E)	Extra Etching Efficiency(%E)	Highest, Average Cell Efficiency (%E)
300 µL SWCNTs	72	187	7	-	7.5, 7 ± 0.63
300µL SWCNTs +400µL MoS_2 (1)	65	376	8	7.5 (15 sec)	8.62, 8.04 ± 0.03
300µL SWCNTs +400µL MoS_2 (2)	65	351.2	8	7 (30 sec)	
300µL SWCNTs +400µL MoS_2 (3)	67	297	8.62	6.5 (45 sec)	

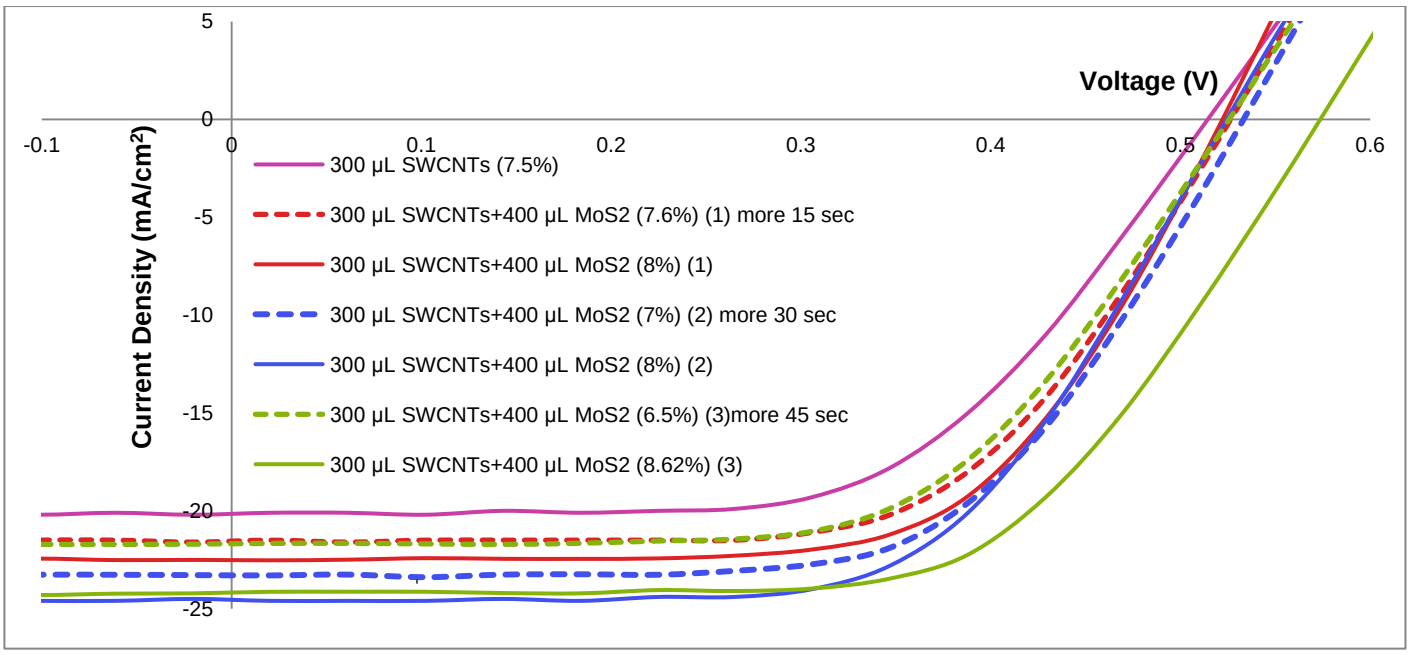

Figure (38): Light curves (J-V curves) for the normal time 2% HF etching treatments hybrid MoS_2 (400µL) and SWCNTs (300µL) solar cells (solid lines), and the different time 2% HF etching treatments more 15second for cell (1), 30second for cell (2) and 45seconds for cell (3) hybrid MoS_2 (400µL) and SWCNTs (300µL) solar cells (dashed lines).

Table (4): The parameters of the best efficiency hybrid MoS_2/SWCNTs-n-Si solar cells with the normal 2% HF etching treatment time (short circuit current J_{sc} (mA/cm^2), open circuit voltage V_{oc} (V), Fill Factors (FF), Efficiency %, current shunt resistance R_{shunt} (Ohms), and series resistance R_{series} (Ohms).

Cell Name	J_{sc} (mA/cm^2)	V_{oc}(V)	FF	R_{shunt} (Ohms)	R_{series} (Ohms)
300 µL SWCNTs	24.114	0.515	0.6	5.29E+03	1.05E+02
300µL SWCNTs+400µL MoS_2 (1)	22.517	0.523	0.63	2.34E+04	7.12E+01
300µL SWCNTs+400µL MoS_2 (2)	24.556	0.524	0.61	6.94E+03	7.55E+01
300µL SWCNTs+400µL MoS_2 (3)	24.177	0.573	0.62	6.54E+03	8.12E+01

Ratio experiment

As mentioned before, CNTs-n-Si based solar cells were prepared to be ready for the comparison with the new sort of solar (MoS_2/SWCNTs hybrid) cells. A control solar cell of pristine 300µL SWCNTs was prepared and yielded an average efficiency of ~7% with a high transmittance of ~73% and an average of low sheet resistance193$(\Omega.\mathrm{cm}^{-1})$ (see Table (A1 and A2) in the Appendix for all information about SWCNTs solar cells). In this experiment, the ratio experiment, a complete series of chemically exfoliated hybrid molybdenum disulfide/single wall carbon nanotubes solar cells were fabricated by changing the volume of MoS_2 (100, 200, 300, 400, 500, 600, 700, 800, 900, and 1000µL) added to a control volume of SWCNTs (300µL). The depletion region could be created between the MoS_2 (n-semiconductor) and SWCNTs (p-semiconductor) and this results in p-n junction solar cells.

The experimental data is written in detail in the Appendix (The average sheet resistivity in Table (A1), the average parameters of the solar cells (short circuit current J_{sc}(mA/cm^2), open circuit voltage V_{oc}(V), fill factor (FF), efficiency%, current shunt resistance R_{shunt} (Ohms), and series resistance R_{series} (Ohms) in Table (A2). Tables (5) and (6) display the highest solar cell efficiency with their parameters. Their corresponding J-V curves were plotted in Figure (41). From the data, it can be noticed that when adding MoS_2, the efficiency increased for the volumes (100-600µL) by almost ~30% but from 700 to 1000µL it seemed to be decreasing but by a modest ratio ~20%. In other words, the efficiency of the hybrid MoS_2/SWCNTs solar cells was higher than the pristine SWCNTs solar cells by ~30% see Figure (39).

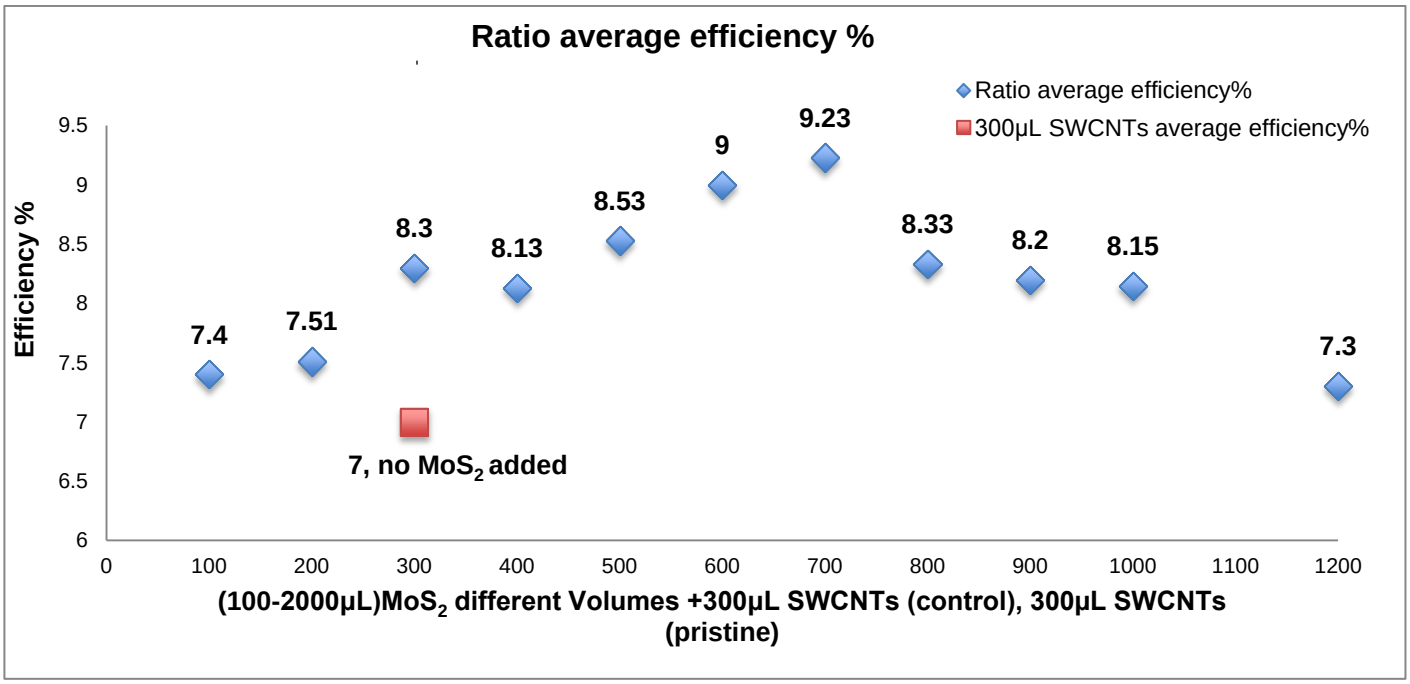

Figure (39): The average efficiency values for the ratio experiment, hybrid (100-2000µL) MoS_2 different volume+ (300µL) SWCNTs (control), (300µL) SWCNTs (pristine).

The optical properties of the cells (transmittance) at first did not change that much even when up to half mL of MoS_2. However, after that the transparency of the rest of the series began to present a noticeable drop, this was because the films got thicker and reduced the light getting through to the Si substrate. The sheet resistivity for the entire series showed a decline from 460.1 to 266.2($\Omega.\,cm^{-1}$) and then increased up to 352.1($\Omega.\,cm^{-1}$) for 300µL SWCNTs +1000µL MoS_2. The sheet resistivity should show an increasing or decreasing trend but here it did not. This could be because two different batches were prepared at different times so the sonication time for the stock solutions were different and the amount or the number of layers was different. Compared to the pristine SWCNTs the sheet resistance improved significantly by almost double the value or more as shown in Figure (40).

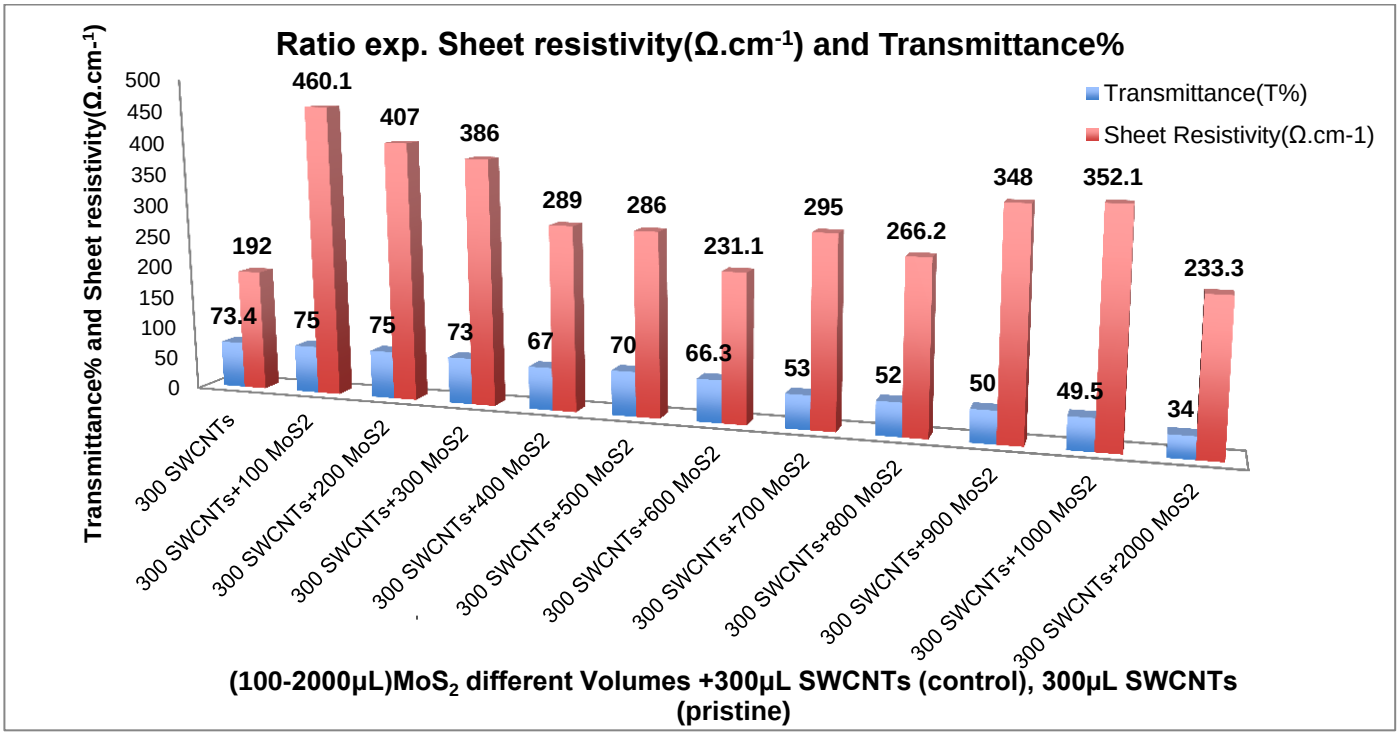

Figure (40): The relationship between the Transmittance% and Sheet resistivity($\Omega.\,cm^{-1}$) as a factor of increasing the MoS_2volumes, 300µL SWCNTs (pristine).

The short circuit current (J_{sc}) revealed an average of ~22 (mA/cm^2), which was similar to the CNTs cell. The highest currents 24.642 and 25.544(mA/cm^2) were for 300µL SWCNTs+200µL MoS_2 and 300µL SWCNTs+600µL of MoS_2 respectively. The open circuit voltage (V_{oc}) overall represented a significant increase from 0.527 to 0.575 and did also grew when compared to the control sample of SWCNTs by 48%. Other important parameter that implies the quality of a solar cell is the fill factor (FF). The presence of the MoS_2 improved the fill factor roughly by 20% when compared to the control sample of SWCNTs, where, the highest one was for 300µL SWCNTs+2mL MoS_2 with a value of 0.73 in contrast the CNT only fill factor, which was 0.53. To sum up, the efficiency was highest for 300µL SWCNTs+600µL MoS_2 (9.8%) and drops for 300µL SWCNTs+1000µL MoS_2 (7.4%). The variations in the efficiency trend could be because the efficiency influenced by many factors: the transmittance, sheet resistivity and fill factors. Furthermore, as mentioned before the fill factors increased generally whereas, the sheet resistivity for the complete series seemed to be decreasing (increasing the conductivity). Although, because the transparency fell down to ~50% with more material addition, the efficiency dropped. Not just that the films became certainly thick as the materials' volumes increased. Another important point is that, when adding more MoS_2 and hybridised it with CNTs in order to distinguish the effect, via expanding the ratio to 1:10. That came out with a cell with an efficiency of 7.7% for 300µL SWCNTs+2mL MoS_2 whereas, the pristine SWCNTs was 7.5% that really close. The

transmittance declined to 34% while the sheet resistivity increased to 233.3($\Omega.\,cm^{-1}$). However, the open circuit voltage and fill factor improved by more than ~30% (0.545 and 0.73) for the 300µL SWCNTs+2mL MoS_2 respectively in contrast to the pristine SWCNTs solar cell. The final words, the addition of the molybdenum disulfide (MoS_2) had improved the performance and quality of the solar cells as expected as a contrast with the pristine single wall carbon nanotubes. The improvement in the efficiency for the hybrid MoS_2/SWCNTs solar cells was affected by the enhancements of both the open circuit voltage, short circuit current and fill factor, which are substantial factors for the solar cells.

Table (5): The hybrid MoS_2/SWCNTs-n-Si solar cells with, various volume filtrations of MoS_2 (100-2000µL) and controlled volume of SWCNTs 300µL and their parameters (Transmittance (T%), Sheet Resistivity($\Omega.\,cm^{-1}$), and Efficiency (%E)).

Cell Name	Transmittance (T%)	Sheet Resistivity ($\Omega.\,cm^{-1}$)	Average Cell Efficiency(%E)	Highest Cell Efficiency(%E)
300µL SWCNTs	73.4	192	7 ± 0.63	7.5
300µL SWCNTs+100µL MoS_2	75	460.1	7.4 ± 0.07	7.5
300µL SWCNTs+200µL MoS_2	75	407	7.51 ± 0.18	7.74
300µL SWCNTs+300µL MoS_2	73	386	8.3 ± 0.18	8.4
300µL SWCNTs+400µL MoS_2	67	289	8.13 ± 0.45	8.5
300µL SWCNTs+500µL MoS_2	70	286	8.53 ± 0.17	8.7
300µL SWCNTs+600µL MoS_2	66.3	231.1	9 ± 0.58	9.8
300µL SWCNTs+700µL MoS_2	53	295	9.23 ± 0.09	9.33
300µL SWCNTs+800µL MoS_2	52	266.2	8.33 ± 0.47	8.99
300µL SWCNTs+900µL MoS_2	50	348	8.2 ± 0.15	8.73
300µL SWCNTs+1000µL MoS_2	49.5	352.1	8.15 ± 0.54	7.4
300µL SWCNTs+2mL MoS_2	34	233.3	7.3 ± 0.29	7.7

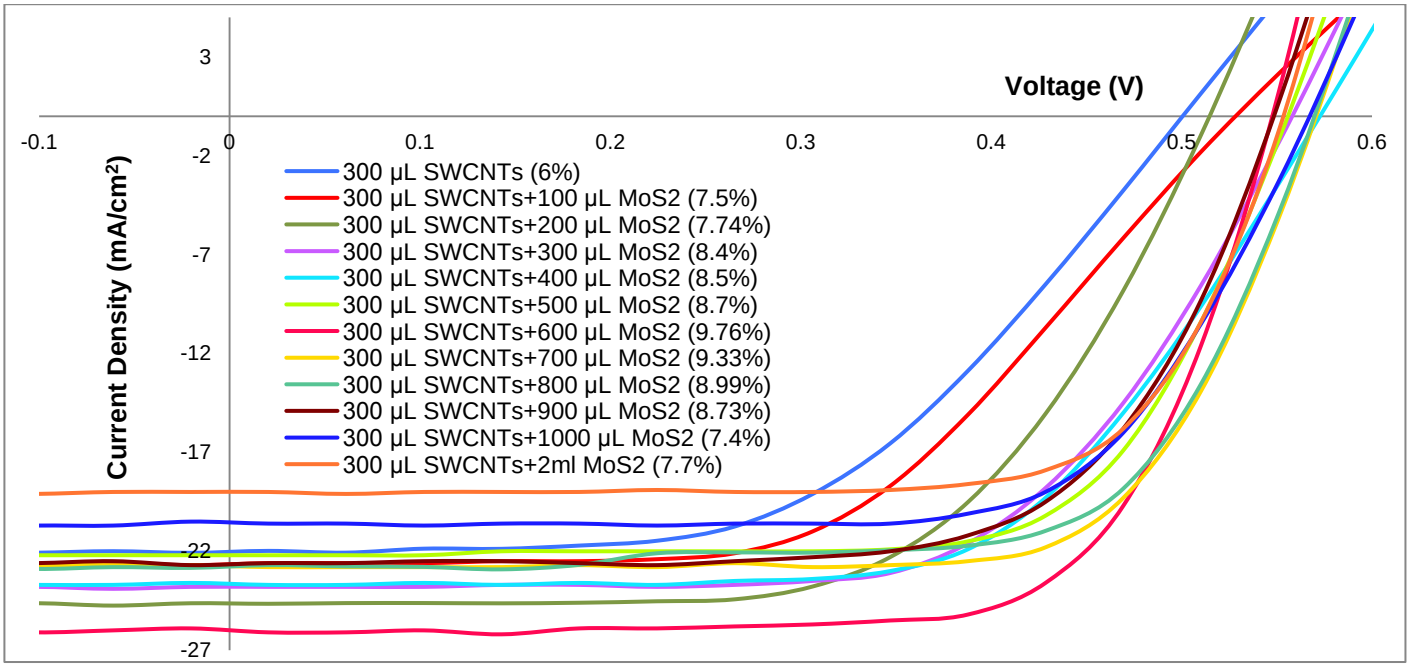

Figure (41): Light curves (J-V curves) for the different ratio hybrid MoS_2 (100-1000µL) and control SWCNTs (300µL) solar cells.

Table (6): The parameters of the best efficiency for the hybrid MoS_2/SWCNTs-n-Si solar cells (Short circuit current J_{sc} (mA/cm^2), Open circuit voltage V_{oc} (V), Fill Factors (FF), Efficiency (%), Current shunt resistance R_{shunt} (Ohms), and Series resistance R_{series} (Ohms).

Cell Name	J_{sc}(mA/cm^2)	V_{oc}(V)	FF	R_{shunt} (Ohms)	R_{series} (Ohms)
300µL SWCNTs	22.029	0.501	0.53	4.81E+03	7.53E+01
300µL SWCNTs+100µL MoS_2	22.615	0.527	0.54	7.31E+03	1.18E+02
300µL SWCNTs+200µL MoS_2	24.642	0.515	0.61	1.89E+04	6.56E+01
300µL SWCNTs+300µL MoS_2	23.803	0.559	0.63	2.39E+04	7.15E+01
300µL SWCNTs+400µL MoS_2	23.629	0.573	0.63	6.72E+03	8.01E+01
300µL SWCNTs+500µL MoS_2	22.199	0.556	0.7	2.55E+04	5.60E+01
300µL SWCNTs+600µL MoS_2	25.544	0.522	0.61	7.57E+03	5.84E+01
300µL SWCNTs+700µL MoS_2	22.743	0.575	0.71	3.80E+03	5.91E+01
300µL SWCNTs+800µL MoS_2	22.771	0.574	0.69	3.73E+03	5.98E+01
300µL SWCNTs+900µL MoS_2	22.62	0.548	0.68	4.53E+03	5.17E+01
300µL SWCNTs+1000µL MoS_2	20.55	0.575	0.7	2.41E+04	7.16E+01
300µL SWCNTs+2mL MoS_2	19.031	0.554	0.73	4.62E+04	5.33E+01

Thickness experiment

In this experiment, the film thickness was changed by varying the amount of both the MoS_2 (200, 400, 800, 1200, 1500 and 1800µL) and SWCNTs (150, 300, 600, 900, 1200 and 1500µL) but the ratio of the two stock solutions was kept the same at 3:4. The varying in the film thickness resulted in changes in the film colour as depicted in Figure (42).

Figure (42): The changes in the film colour according to the changes in the film thickness when filtering different volume of both MoS_2 (200-1800µL) and SWCNTs (150-1500µL).

The best cells' performance data are in Tables (7) and (8); their corresponding J-V curves are in Figure (45). The entire experimental data including the average sheet resistivity, average cell efficiency, and the average of the solar cell parameters are in detail in Tables (A6), and (A7) in the Appendix. The control sample was 300µL SWCNTs+400µL MoS_2 since it generated the highest efficiency ~8.7%, then half of this amount was fabricated and double and then triple. The colour became darker correlated with the increasing in the film thickness by adding more material. The film was really thin with very high transparency 88.5% for 150µL SWCNTs+200µL MoS_2 and shifted to a noticeable dark black thick film with low transparency 21% 1500µL SWCNTs+1800µL MoS_2 as additional volumes of the suspension were used. Though for the first thickness film (150µL SWCNTs+200µL MoS_2), the solar cell electrode had a high transmittance conversely the cell still did not yield a high efficiency (5.02%). This was because the amount of MoS_2 and SWCNTs was not enough (very little volume filtrations). SEM images Figure (29 a) were obtained and showed that the materials

did not cover all the silicon substrate. Consequently, there were several areas where there was no material in addition to other areas where the film was really thin. This could result in the creation of a poor depletion region between the CNTs and the Si substrate or might be between the MoS_2 and SWCNTs. However, since the filtered volumes were really small, the MoS_2 did not show its effects along with a high value of sheet resistivity ~708$(\Omega.\,cm^{-1})$ and that indicated low conductivity and fill factor of 0.35 that result in poor efficiency. Moreover, the remainder of the series exhibited a decreasing trend in the efficiency from ~8% for 300µL SWCNTs+400µL MoS_2 in average down to ~2% for 1500µL SWCNTs+1800µL MoS_2 as shown in Figure (43).

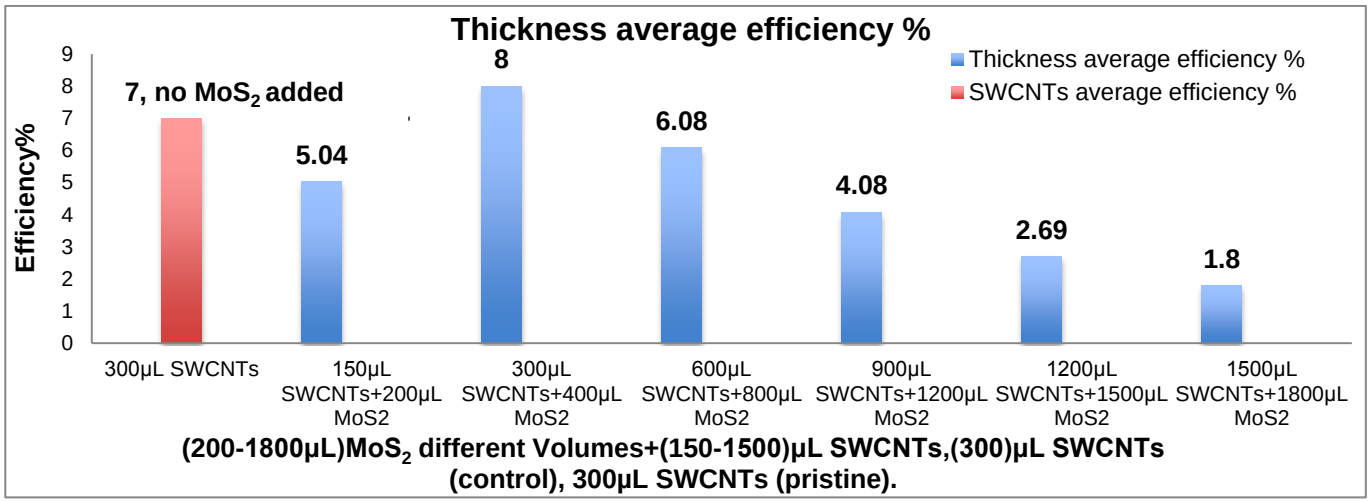

Figure (43): The average efficiencies for the thickness experiment, the MoS_2 (200, 400, 800, 1200, 1500 and 1800µL) and SWCNTs (150, 300, 600, 900, 1200 and 1500µL), (300µL) SWCNTs (pristine).

Similarly, for the sheet resistivity from ~708$(\Omega.\,cm^{-1})$ decreased down to ~50$(\Omega.\,cm^{-1})$, as well as the transmittance fell down from 88.5% to 21%. Thus, both transmittance and sheet resistivity gave a decreasing trend, which is normal; as the films get thicker with more solutions added, see Figure (44).

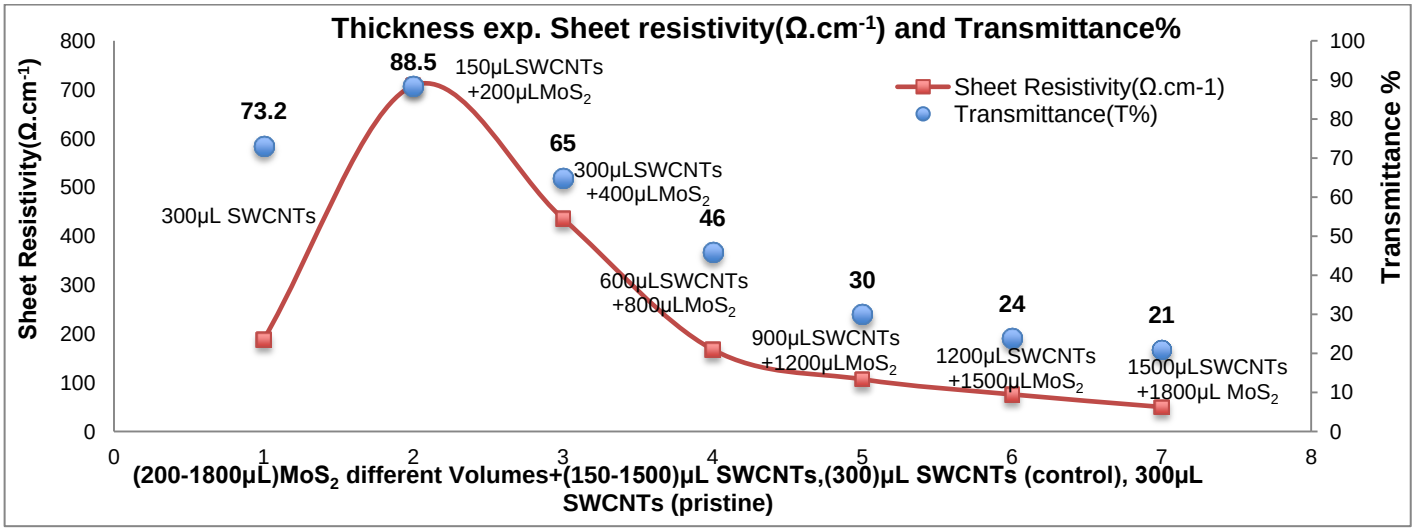

Figure (44): The relationship between the Transmittance% and Sheet resistivity $(\Omega.\,cm^{-1})$ as a factor of increasing the film thickness, (300µL) SWCNTs (pristine).

Along with the short circuit current, which fell from 26.497 to 6.05 (mA/cm^2), the fill factor showed an overall increase with thickness 0.35 to 0.71. Whilst, the open circuit voltage did not exhibit a regular increasing or decreasing trend, the highest values were 0.551 and 0.545 for 150µL SWCNTs+200µL MoS_2 and 900µL SWCNTs+1200µL MoS_2 respectively. Undeniably, the reason why the solar cells had a low PCEs generation was due to the poor optical properties (low Transmittance) as the film got thicker. The transparency dropped and this decreased the light of getting through the materials which did not give back a desired efficiency along with other parameters that play an important role in the cells performance and quality.

Table (7): The hybrid MoS_2/SWCNTs-n-Si solar cells with, various filtrations thickness of MoS_2 (200-1800µL) and of SWCNTs (150-1500µL) with the same ratio (1:2) and their parameters (Transmittance (T%), Sheet Resistivity ($\Omega.\dot{c}m^{-1}$), and Efficiency (%E)).

Cell Name	Transmittance (T%)	Sheet Resistivity ($\Omega.\dot{c}m^{-1}$)	Average Cell Efficiency (%E)	Highest Cell Efficiency (%E)
300µL SWCNTs	73.2	188.3	7 ± 0.63	7.5
150µL SWCNTs+200µL MoS_2	88.5	708.1	5.04 ± 0.12	5.02
300µL SWCNTs+400µL MoS_2	65	436.1	8 ± 0.52	8.7
600µL SWCNTs+800µL MoS_2	46	168.1	6.08 ± 0.11	6.24
900µL SWCNTs+1200µL MoS_2	30	107	4.08 ± 0.12	4.2
1200µL SWCNTs+1500µL MoS_2	24	76	2.69 ± 0.04	2.73
1500µL SWCNTs+1800µL MoS_2	21	50.2	1.80 ± 0.01	1.81

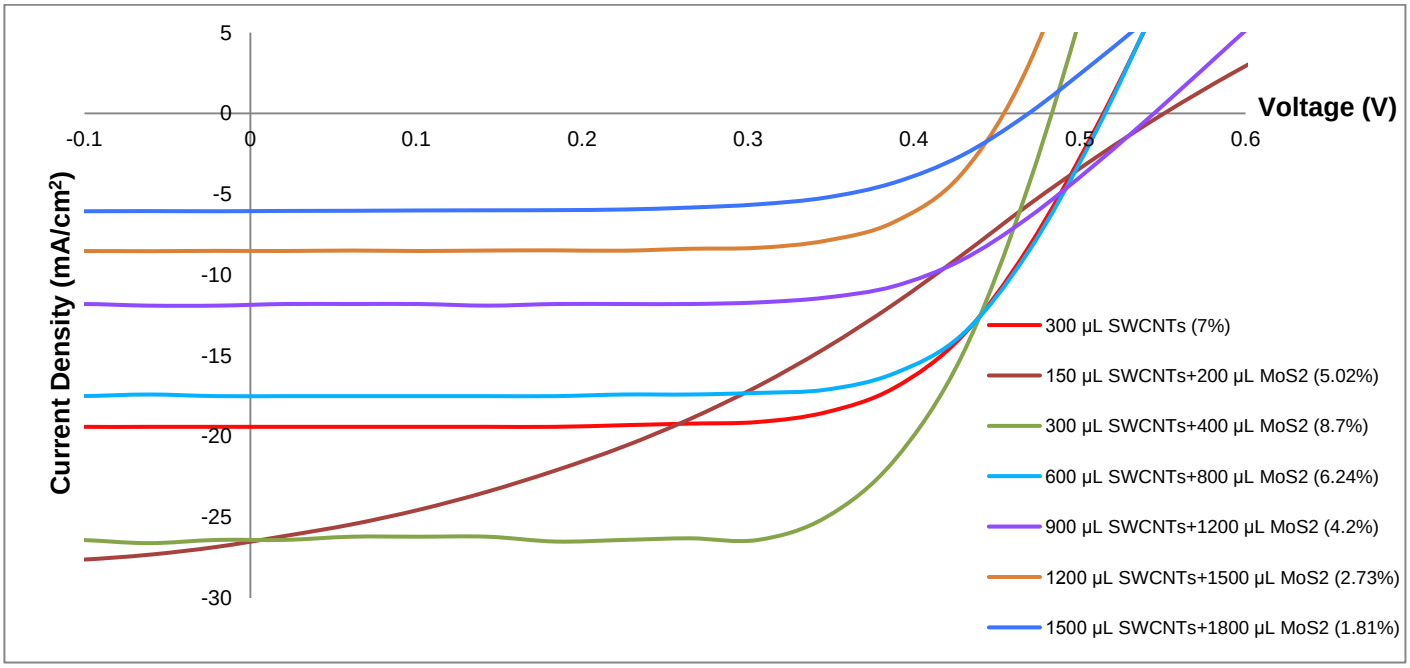

Figure (45): Light curves (J-V curves) for the different films' thickness hybrid MoS_2 (200-1800µL) and SWCNTs (150-1500µL) solar cells.

Table (8): The parameters of the best efficiency for the hybrid MoS_2/SWCNTs-n-Si solar cells with different thickness (Short circuit current J_{sc} (mA/cm^2), Open circuit voltage V_{oc} (V), Fill Factors (FF), Efficiency %, Current shunt resistance R_{shunt} (Ohms), and Series resistance R_{series} (Ohms).

Cell Name	J_{sc} (mA/cm^2)	V_{oc}(V)	FF	R_{shunt} (Ohms)	R_{series} (Ohms)
300µL SWCNTs	19.387	0.515	0.66	6.75E+04	6.92E+01
150µL SWCNTs+200µL MoS_2	26.497	0.551	0.35	7.69E+02	1.90E+02
300µL SWCNTs+400µL MoS_2	26.38	0.487	0.67	1.16E+04	4.95E+01
600µL SWCNTs+800µL MoS_2	17.489	0.516	0.69	6.87E+04	6.90E+01
900µL SWCNTs+1200µL MoS_2	11.846	0.545	0.65	1.63E+04	1.41E+02
1200µL SWCNTs+1500µL MoS_2	8.516	0.451	0.71	6.02E+04	7.73E+01
1500µL SWCNTs+1800µL MoS_2	6.05	0.47	0.64	2.28E+04	2.00E+02

Layered experiment

With the previous impressive results in this project where the highest efficiency reported for the first time when using mixture of molybdenum disulfide and single wall carbon nanotubes in n-type silicon solar cells was ~9.8%, another new design of the device was established hoping to get higher efficiency since there was a huge potential for efficiency improvement where in this innovative experiment a layer of MoS_2 and another layer of SWCNTs were filtered on top of each other via vacuum filtration. The first layer was MoS_2 film using different volume filtrations (100-1000µL) then another film of controlled volume (300µL SWCNTs) was applied over the previous film. Here, the depletion region could be created between the SWCNTs as p-type semiconductor and Si substrate as n-type semiconductor as the MoS_2 film was thin hence; the CNTs can possibly reach the Si substrate. As the as the MoS_2 film got thicker the CNTs might not contact the Si substrate, the depletion region could be created between the MoS_2 and SWCNTs. Since, this experiment is new further studies are needed in order to get an answer about this experiment behaviour. All the experimental details are in Tables from (A8) to (A9) in the Appendix where the highest solar cells efficiency with their parameters are mentioned in Tables (9) and (10) and their corresponding J-V curves are plotted in Figure (48). Overall, the experiment outcomes were better than the ratio experiment data, except the transmittance was observed to be decreasing from 66 to 55% compared to the control MoS_2 cell sample 85% by ~30%. Furthermore, those cells have low sheet resistivity values and high conductivity values which yielded an overall increasing in the efficiency values compared to the ratio experiment for the complete series as shown in Figure (46).

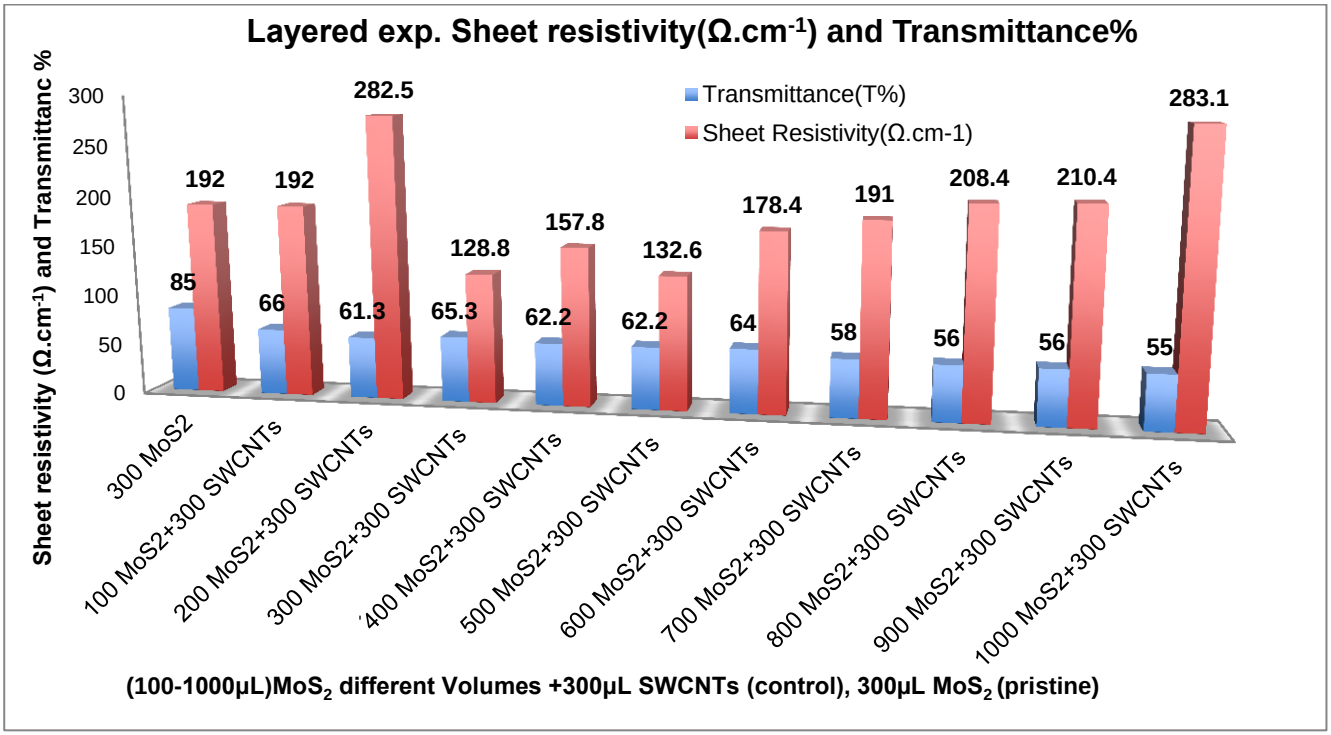

Figure (46): The relationship between the Transmittance% and Sheet resistivity ($\Omega.\,cm^{-1}$) as a factor of increasing the MoS_2 volumes, 300µL MoS_2 (pristine).

However, the efficiency of the cells was promising. The highest value was ~10.2% for 600µL MoS_2+300µL SWCNTs compared to the pure MoS_2 cell 0% and this was unprecedented value when using MoS_2. The 0% for MoS_2 is expected as the MoS_2 an n-type semiconductor and the Si substrate is n-type which indicated there was no deletion region. While, the lowest efficiency was 7.8% for 1000µL MoS_2 +300µL SWCNTs, and still higher than the pristine MoS_2 as shown in Figure (47).

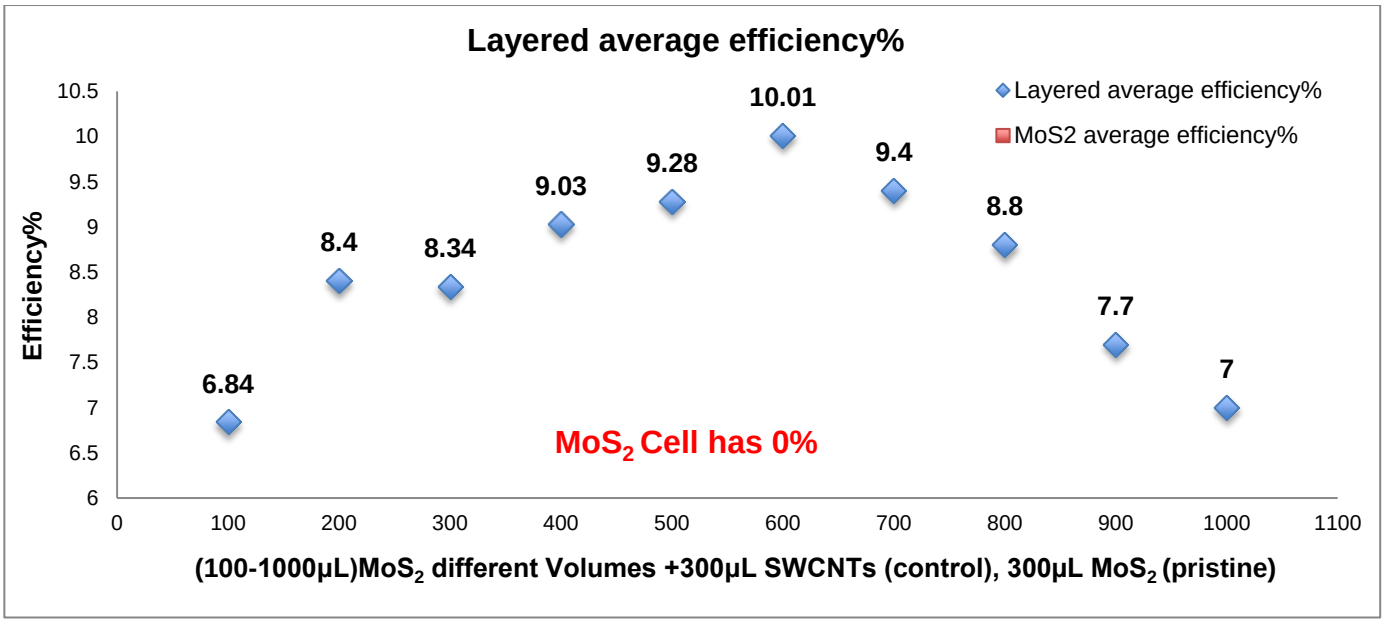

Figure (47): The average efficiency values for the layered experiment, (100-1000 µL) MoS_2+ (300µL) SWCNTs (control), (300µL) MoS_2 (pristine).

The J_{sc} was between 21 to 24(mA/cm^2), the V_{oc} displayed an overall increase and was the highest at 0.575(V) for 600µL MoS_2+300µL SWCNTs. Similarly the fill factor showed a noticeable overall increase. The best value was 0.74 for both 600 and 700µL MoS_2+300µL SWCNTs. Whilst, the sheet resistivity for the control MoS_2 sample was the same as100µL MoS_2+300µL SWCNTs after that the series revealed an overall increase up to 283.1($\Omega.\,cm^{-1}$) for 1000µL MoS_2 +300µL SWCNTs. To summarise, the efficiency of the series increased from 6.91 to 10.2% for 100µL MoS_2+300µL SWCNTs and 600µL MoS_2+300µL SWCNTs respectively, and afterward decreased from 10.2 to 7.8% for the 600µL MoS_2+300µL SWCNTs and 1000µL MoS_2+300µL SWCNTs respectively. Essentially, this could be because the drop in the transparency and conductivity both influenced the cells' PCEs. Additionally, the films became thicker as extra material was added. Finally, there were improvements in all cells' efficiency for this series in comparison to the ratio's series beside the outstanding reported values of low sheet resistivity (high conductivity), high fill factors, short circuit currents, and open circuit voltages along with optimum transmittance values. In fact, the enhancements in the layered experiment in terms of the efficiency were proportional to the improvements in the J_{sc}, V_{oc} and FF.

Table (9): The layers MoS_2/SWCNTs-n-Si solar cells with, various volume filtrations of MoS_2 (100-600µL) and controlled volume of SWCNTs (300µL) and their parameters (Transmittance (T%), Sheet Resistivity ($\Omega.\,cm^{-1}$), and Efficiency (%E)).

Cell Name	Transmittance (T%)	Sheet Resistivity ($\Omega.\,cm^{-1}$)	Average Cell Efficiency (%E)	Highest Cell Efficiency (%E)
300µL MoS_2	85	192	0	0
100µL MoS_2+300µL SWCNTs	66	192	6.84 $\pm$ 0.06	6.91
200µL MoS_2+300µL SWCNTs	61.3	282.5	8.4 $\pm$ 0.58	9.19
300µL MoS_2+300µL SWCNTs	65.3	128.8	8.34 $\pm$ 0.2	8.6
400µL MoS_2+300µL SWCNTs	62.2	157.8	9.03 $\pm$ 0.72	9.56
500µL MoS_2+300µL SWCNTs	62.2	132.6	9.28 $\pm$ 0.27	9.52
600µL MoS_2+300µL SWCNTs	64	178.4	10.01 $\pm$ 0.22	10.2
700µL MoS_2+300µL SWCNTs	58	191	9.4 $\pm$ 0.11	9.5
800µL MoS_2+300µL SWCNTs	56	208.4	8.8 $\pm$ 0.54	9.3
900µL MoS_2+300µL SWCNTs	56	210.4	7.7 $\pm$ 0.61	8.24
1000µL MoS_2+300µLSWCNTs	55	283.1	7 $\pm$ 0.62	7.8

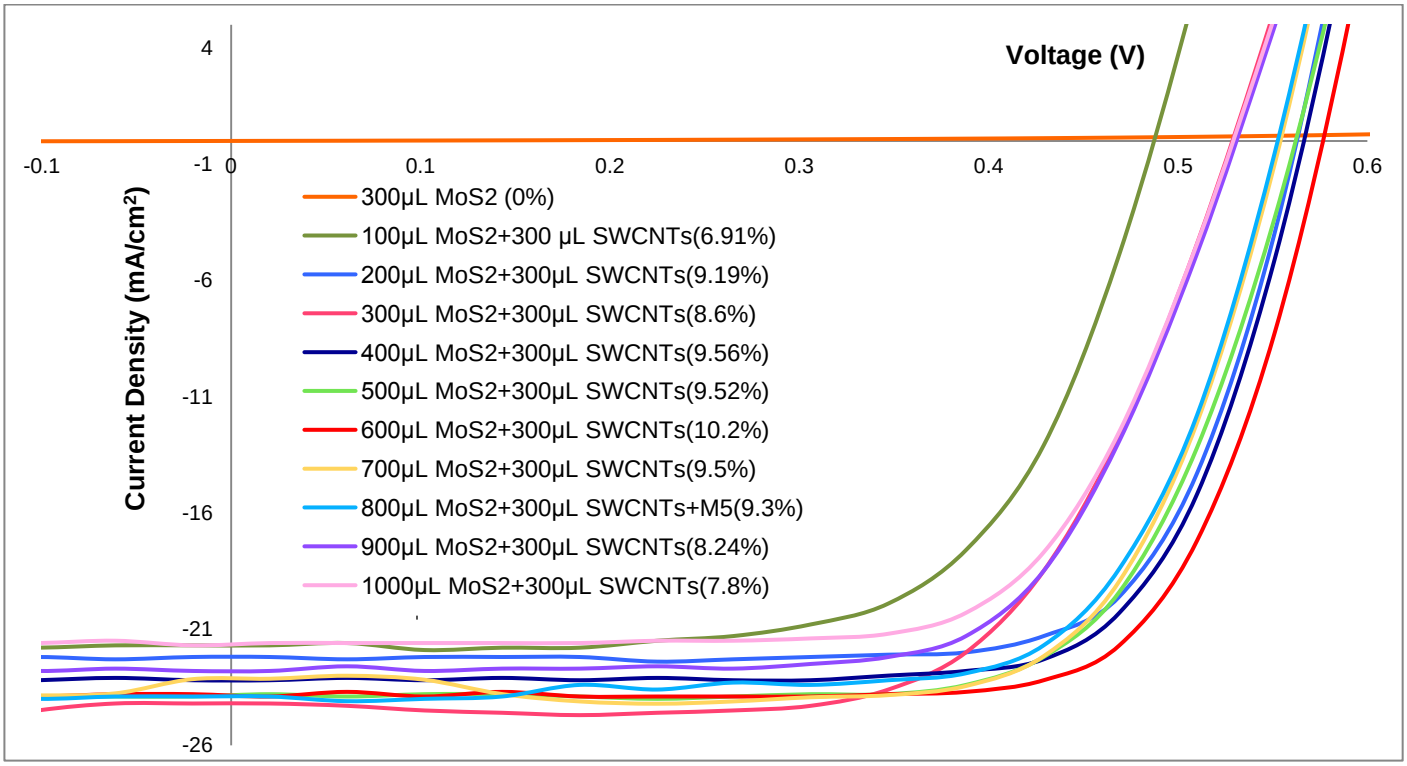

Figure (48): Light curves (J-V curves) for the layer films MoS_2 (100-1000µL) and control layer films of SWCNTs (300µL) solar cells.

Table (10): The parameters of the best efficiency hybrid films layers of MoS_2/SWCNTs SWCNTs-n-Si solar cells (Short circuit current J_{sc} (mA/cm^2), Open circuit voltage V_{oc} (V), Fill Factors (FF), Efficiency (%), Current shunt resistance R_{shunt} (Ohms), and Series resistance R_{series} (Ohms).

Cell Name	J_{sc} (mA/cm^2)	V_{oc}V)	FF	R_{shunt} (Ohms)	R_{series} (Ohms)
300µL MoS_2	-0.001	-0.007	-4.58	8.51E+04	8.92E+04
100µL MoS_2+300µL SWCNTs	21.673	0.494	0.65	1.35E+05	6.28E+01
200µL MoS_2+300µL SWCNTs	22.203	0.567	0.73	1.44E+04	4.97E+01
300µL MoS_2+300µL SWCNTs	24.207	0.532	0.66	3.10E+04	6.27E+01
400µL MoS_2+300µL SWCNTs	23.206	0.572	0.72	3.40E+06	5.14E+01
500µL MoS_2+300µL SWCNTs	23.838	0.565	0.71	2.07E+04	5.24E+01
600µL MoS_2+300µL SWCNTs	23.841	0.575	0.74	4.95E+03	3.66E+01
700µL MoS_2+300µL SWCNTs	23.144	0.555	0.74	2.75E+04	4.64E+01
800µL MoS_2+300µL SWCNTs	23.894	0.553	0.7	9.01E+03	4.58E+01
900µL MoS_2+300µL SWCNTs	22.762	0.535	0.68	5.06E+04	6.42E+01
1000µL MoS_2+300µL SWCNTs	21.609	0.533	0.68	4.51E+03	6.43E+01

Figure (49), depicts the best J-V curves for both ratio and layered experiments where the best J-V curve was plotted from each experiment and their corresponding parameters in Table (11). From the ratio experiment the J-V curve for the cell with volume filtration of 300µL SWCNTs+600µL MoS_2 with an efficiency of 9.76% while from the layered experiment the J-V curve with the volume filtration of 600µL MoS_2+300µL SWCNTs with efficiency of 10.2%. As well as the J-V curves for both pristine SWCNTs and MoS_2 with the volume filtrations of

300µL for both which produced an efficiencies of 6% and 0% respectively. However, when adding more material of MoS_2 (2mL) to the SWCNTs the efficiency went down to 7.7%. To close, the addition of MoS_2 to the SWCNTs improved the CNTs-n-silicon solar cell's efficiency by ~40% when compared to the pristine CNTs solar cells while by 100% when compared to the pristine MoS_2 solar cells.

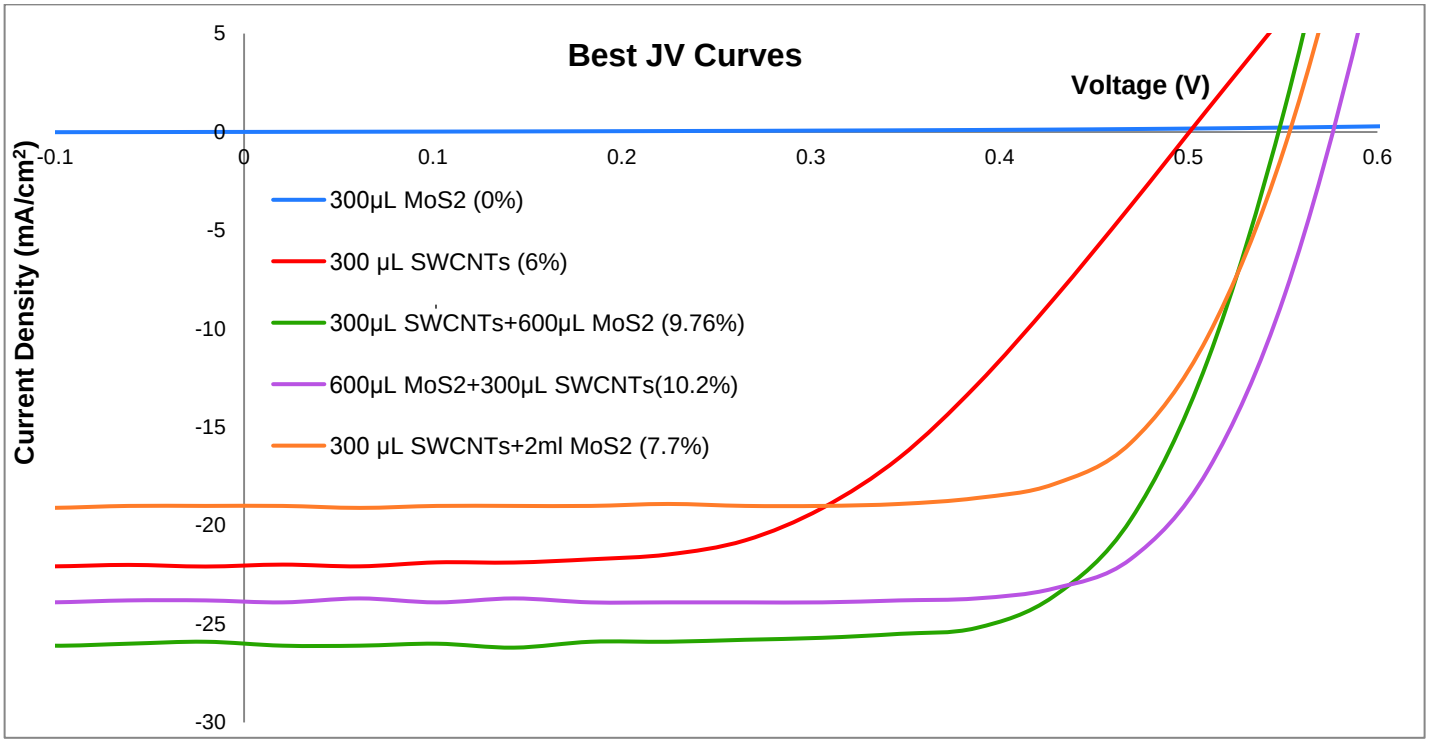

Figure (49): Best J-V curves from experiments (Ratio, Layered) in comparison with pure SWCNTs and MoS_2.

Table (11): The best solar cells' performance parameters for both ratio and layered experiments.

Cell Name	Transmittance (T%)	Sheet Resistivity ($\Omega.\,cm^{-1}$)	Average Cell Efficiency (%E)	Highest Cell Efficiency (%E)	J_{sc} (mA/ cm^2)	V_{oc}(V)	FF
300µL MoS_2	85	192	0	0	-0.001	-0.007	-4.58
300µL SWCNTs	73.4	192	7 ± 0.63	7.5	22.029	0.501	0.53
300µLSWCNTs +600µL MoS_2	66.3	231.1	9 ± 0.58	9.8	25.544	0.522	0.61
600µLMoS_2 +300µL SWCNTs	64	178.4	10.01 ± 0.22	10.2	23.841	0.575	0.74
300µLSWCNTs +2mL MoS_2	34	233.3	7.3 ± 0.29	7.7	19.031	0.554	0.73

Chapter 4:

Conclusions

In summary, molybdenum disulfide has been successfully synthesised using lithium intercalation (Li_xMoS_2) (chemically exfoliation) of the bulk form of MoS_2 to form flakes. Different instruments such as AFM, SEM and Raman were used to characterise all MoS_2, SWCNTs and hybrid MoS_2/SWCNTs in order to measure the molybdenum disulfide flakes' thickness and width, and showed the hybrid MoS_2/SWCNTs. The MoS_2 flakes found to be on average ~ (1nm –100nm) thick with lateral dimensions on the order of ~100-500nm as observed from the AFM and SEM which were both used to investigate the existence of the materials. Raman spectroscopy exhibited the existence of MoS_2 characteristics peaks at ~385cm^{-1} and ~405cm^{-1} that indicated the E^1_{2g}, and A_{1g} vibrations modes which were for the in plane and out of plane vibrations respectively and agreed with literature. Likewise, for SWCNTs peaks which appeared at the ~162cm^{-1}, ~1332cm^{-1}, and ~1587cm^{-1} and that defined the radial breathing modes (RBMs) at low frequencies, D-band, and G-band at high frequencies respectively. Certainly, both AFM and Raman techniques prove that the MoS_2 in this work was few layers as compared with literature. Subsequently, three sorts of solar cells were fabricated, the SWCNTs-n-type silicon solar cells, the hybrid MoS_2/SWCNTs-n-type silicon solar cells with different volume filtrations and finally, the layered MoS_2/SWCNTs-n-type silicon solar cells. The average efficiency obtained from the pristine CNTs cells was ~7$\pm$0.63% whereas, the highest efficiency after the addition of MoS_2 to the SWCNTs was 10.01$\pm$0.22% and that advanced the solar cell performance by at least 40%. Thus, the addition of molybdenum disulfide has enhanced the SWCNTs-n-silicon based solars performance.

Future work

The layered SWCNTs/MoS_2 -Si solar cells as shown in Figure (50) could be prepared. At first the SWCNTs film will be attached and then another MoS_2 film will be attached over the SWCNTs film. That will be prepared by filtering different volume filtrations of SWCNTs (100-1000μL) and then at the same time a filtering control volume of MoS_2 (600μL) as a second layer since this produced the best efficiency~ 10% via vacuum filtration method. In order to distinguish the differences between those cells the layered SWCNTs/MoS_2 and the layered MoS_2/SWCNTs-n-silicon solar cells and their efficiency will be compared.

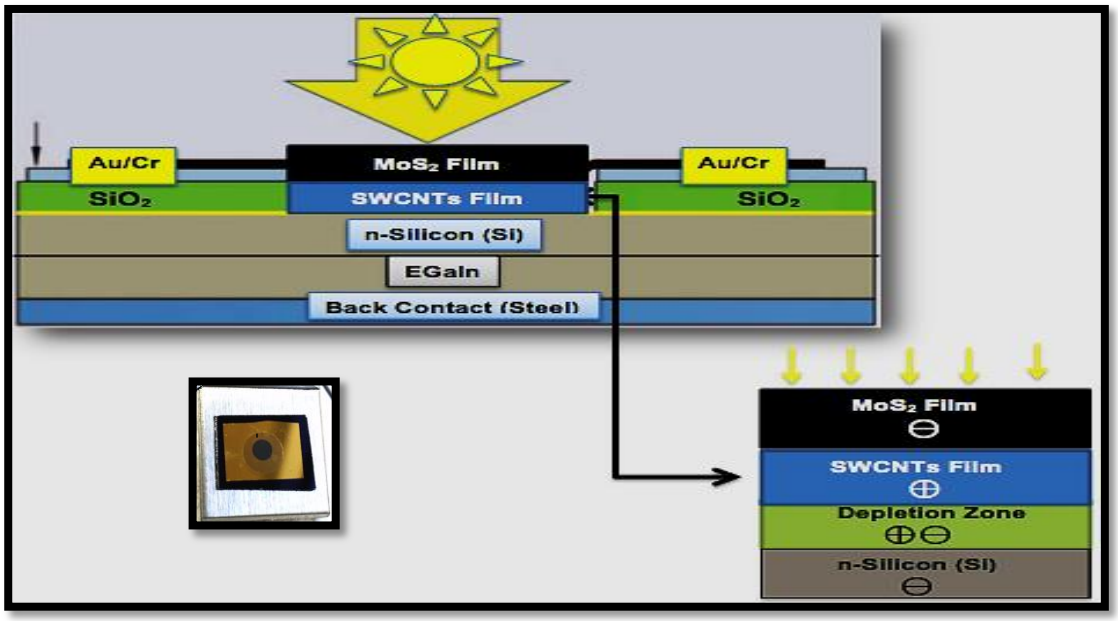

Figure (50): The device fabrication for the layered SWCNTs/MoS_2 n-Si solar cells. [26]

A new photolithography mask produced contained many shapes for the active area (a circle was used in this work without grid). The others are (circles with and without grid, different size), and (square with and without grids with different diameters). Moreover, other work suggests the square appears to generate higher efficiency than the circle consequently this would be worth trying with MoS_2 see Figure (51).

Figure (51): different active area shapes.

Another possible experiment is to carry out is preparing hybrid graphene/molybdenum disulfide/carbon nanotubes because it is crucial to take advantage of the graphene and figure out the effect with molybdenum disulfide. Besides, synthesis the molybdenum disulfide with more controllable methods in order to be able to control the number and orientations of layers such as, chemical vapour deposition could also be investigated.

References

1 Tune, D. D. & Shapter, J. G. Effect of nanotube film thickness on the performance of nanotube-silicon hybrid solar cells. *Nanomaterials* **3**, 655-673 (2013).

2 Foroudastan, S. D. & Dees, O. in *Proceedings of the international conference on renewable energy for developing countries.*

3 Sharma, S., Jain, K. K. & Sharma, A. Solar Cells: In Research and Applications—A Review. *Materials Sciences and Applications* **6**, 1145 (2015).

4 Tsai, M.-L. *et al.* Monolayer MoS_2 heterojunction solar cells. *Acs Nano* **8**, 8317-8322 (2014).

5 Batmunkh, M., Biggs, M. J. & Shapter, J. G. Carbonaceous Dye-Sensitized Solar Cell Photoelectrodes. *Advanced Science* **2** (2015).

6 Tune, D. D., Flavel, B. S., Quinton, J. S., Ellis, A. V. & Shapter, J. G. Single-Walled Carbon Nanotube/Polyaniline/n-Silicon Solar Cells: Fabrication, Characterization, and Performance Measurements. *ChemSusChem* **6**, 320-327 (2013).

7 Bernardi, M. *et al.* Nanocarbon-based photovoltaics. *ACS nano* **6**, 8896-8903 (2012).

8 Tune, D. D. *et al.* The role of nanotubes in carbon nanotube–silicon solar cells. *Advanced Energy Materials* **3**, 1091-1097 (2013).

9 Alturaif, H. A., ALOthman, Z. A., Shapter, J. G. & Wabaidur, S. M. Use of carbon nanotubes (CNTs) with polymers in solar cells. *Molecules* **19**, 17329-17344 (2014).

10 Tune, D. D., Blanch, A. J., Krupke, R., Flavel, B. S. & Shapter, J. G. Nanotube film metallicity and its effect on the performance of carbon nanotube–silicon solar cells. *physica status solidi (a)* **211**, 1479-1487 (2014).

11 Tune, D. D., Flavel, B. S., Krupke, R. & Shapter, J. G. Carbon Nanotube-Silicon Solar Cells. *Advanced Energy Materials* **2**, 1043-1055 (2012).

12 Yu, L., Tune, D., Shearer, C., Grace, T. & Shapter, J. Heterojunction Solar Cells Based on Silicon and Composite Films of Polyaniline and Carbon Nanotubes. *IEEE Journal of Photovoltaics* **6**, 688-695 (2016).

13 Gaur, A. P. *et al.* Surface energy engineering for tunable wettability through controlled synthesis of MoS_2. *Nano letters* **14**, 4314-4321 (2014).

14 Liu, W., Yang, X., Zhang, Y., Xu, M. & Chen, H. Ultra-stable two-dimensional MoS 2 solution for highly efficient organic solar cells. *RSC Advances* **4**, 32744-32748 (2014).

15 Yang, X. *et al.* Engineering crystalline structures of two-dimensional MoS 2 sheets for high-performance organic solar cells. *Journal of Materials Chemistry A* **2**, 7727-7733 (2014).

16 Chung, D. Y. *et al.* Edge-exposed MoS 2 nano-assembled structures as efficient electrocatalysts for hydrogen evolution reaction. *Nanoscale* **6**, 2131-2136 (2014).

17 Tabares, J. O. *et al.* in *Proceedings of.* 115-124.

18 Ahmad, S. & Mukherjee, S. A comparative study of electronic properties of bulk MoS_2 and its monolayer using DFT technique: application of mechanical strain on MoS_2 monolayer. *Graphene* **3**, 52 (2014).

19 Li, X. & Zhu, H. Two-dimensional MoS_2: Properties, preparation, and applications. *Journal of Materiomics* **1**, 33-44, doi:http://dx.doi.org/10.1016/j.jmat.2015.03.003 (2015).

20 Jiang, S.-D. *et al.* Surface functionalization of MoS 2 with POSS for enhancing thermal, flame-retardant and mechanical properties in PVA composites. *RSC Advances* **4**, 3253-3262 (2014).

21 Mak, K. F., Lee, C., Hone, J., Shan, J. & Heinz, T. F. Atomically thin MoS 2: a new direct-gap semiconductor. *Physical Review Letters* **105**, 136805 (2010).

22 Eda, G. *et al.* Photoluminescence from chemically exfoliated MoS_2. *Nano letters* **11**, 5111-5116 (2011).
23 ZIMEI, C. *Preparation of oriented molybdenum disulfide thin films for photoelectrochemical energy havesting applications*, (2014).
24 Cai, Y. *et al.* Easy incorporation of single-walled carbon nanotubes into two-dimensional MoS_2 for high-performance hydrogen evolution. *Nanotechnology* **25**, 465401 (2014).
25 Xu, M. *Carbon nanotubes make molybdenum disulfide more active*, <http://nanotechweb.org/cws/article/lab/59223> (2014).
26 Cui, K. & Maruyama, S. Carbon Nanotube-Silicon Solar Cells: Improving performance for next-generation energy systems. *IEEE Nanotechnology Magazine* **10**, 34-C33 (2016).
27 Cotfas, D. Determining the parameters of solar cell.
28 Aparicio, M. P., Pelegrí-Sebastiá, J., Sogorb, T. & Llario, V. *Modeling of photovoltaic cell using free software application for training and design circuit in photovoltaic solar energy*. (INTECH Open Access Publisher, 2013).
29 Hao, L. *et al.* Electrical and photovoltaic characteristics of MoS_2/Si p-n junctions. *Journal of Applied Physics* **117**, 114502, doi:doi:http://dx.doi.org/10.1063/1.4915951 (2015).
30 Fan, X. *et al.* Fast and efficient preparation of exfoliated 2H MoS_2 nanosheets by sonication-assisted lithium intercalation and infrared laser-induced 1T to 2H phase reversion. *Nano letters* **15**, 5956-5960 (2015).
31 Sundaram, R. *et al.* Electroluminescence in single layer MoS_2. *Nano letters* **13**, 1416-1421 (2013).
32 Jariwala, D. *et al.* Gate-tunable carbon nanotube–MoS_2 heterojunction pn diode. *Proceedings of the National Academy of Sciences* **110**, 18076-18080 (2013).
33 Jeon, I. *et al.* Multilayered MoS 2 nanoflakes bound to carbon nanotubes as electron acceptors in bulk heterojunction inverted organic solar cells. *Organic Electronics* **17**, 275-280 (2015).
34 Ma, D. *et al.* Etching-free transfer of wafer-scale MoS_2 films. *arXiv preprint arXiv:1501.00786* (2015).
35 Graupner, R. Raman spectroscopy of covalently functionalized single-wall carbon nanotubes. *Journal of Raman Spectroscopy* **38**, 673-683 (2007).
36 Hodkiewicz, J. Characterizing carbon materials with Raman spectroscopy. *Thermo Scientific Application Note* **51946** (2010).
37 Jia, Y. *et al.* Encapsulated carbon nanotube-oxide-silicon solar cells with stable 10% efficiency. *Applied Physics Letters* **98**, 133115 (2011).
38 Dettlaff-Weglikowska, U. *et al.* Effect of $SOCl_2$ treatment on electrical and mechanical properties of single-wall carbon nanotube networks. *Journal of the American Chemical Society* **127**, 5125-5131 (2005).
39 Li, Z. *et al.* Light-harvesting using high density p-type single wall carbon nanotube/n-type silicon heterojunctions. *Acs Nano* **3**, 1407-1414 (2009).

Appendices

Table (A1): The average sheet resistivity for the hybrid MoS_2/SWCNTs that filtered using different volume for the MoS_2

Sheet Resistivity ($\Omega.cm^{-1}$)				
Cell Name	Reading 1	Reading 2	Reading 3	Average Readings
300µL SWCNTs	188	193	194	192
300µL SWCNTs+100µL MoS_2	410	465	505.4	460.1
300µL SWCNTs+200µL MoS_2	404.3	408	409.2	407
300µL SWCNTs+300µL MoS_2	380.2	388.3	389	386
300µL SWCNTs+400µL MoS_2	280	285	302	298
300µL SWCNTs+500µL MoS_2	284.3	285	288	286
300µL SWCNTs+600µL MoS_2	204.2	232	257	231.1
300µL SWCNTs+700µL MoS_2	293	293	298	295
300µL SWCNTs+800µL MoS_2	258.2	265	275.4	266.2
300µL SWCNTs+900µL MoS_2	344	346	353.4	348
300µL SWCNTs+1000µL MoS_2	345.3	352	359	352.1
300µL SWCNTs+2mL MoS_2	230	231	239	233.3

Table (A2): The average parameters for the hybrid MoS_2/SWCNTs with different ratio filtrations solar cells

300µL SWCNTs	Cell 1	Cell 2	Cell 3	Average
J_{sc} (mA/cm^2)	22.029	19.387	24.114	21.843
V_{oc} (V)	0.501	0.515	0.515	0.5103
FF	0.53	0.66	0.6	0.60
Efficiency %	6	7	7.5	7
R_{shunt} (Ohms)	5.29E+03	6.75E+04	4.81E+03	2.60E+03
R_{series} (Ohms)	1.05E+02	6.92E+01	7.53E+01	8.32E+01

300µL SWCNTs +100µL MoS_2	Cell 1	Cell 2	Cell 3	Average
J_{sc} (mA/cm^2)	21.186	21.885	22.615	21.895
V_{oc} (V)	0.56	0.555	0.527	0.547
FF	0.62	0.61	0.54	0.59
Efficiency %	7.32	7.38	7.5	7.4
R_{shunt} (Ohms)	1.22E+04	9.23E+03	7.31E+03	9.58E+03
R_{series} (Ohms)	8.77E+01	8.98E+01	1.18E+02	9.85E+01

300µL SWCNTs +200µL MoS_2	Cell 1	Cell 2	Cell 3	Average
J_{sc} (mA/cm^2)	24.542	23.671	24.642	27.285
V_{oc} (V)	0.518	0.51	0.515	0.514
FF	0.57	0.61	0.61	0.60
Efficiency %	7.3	7.5	7.74	7.51
R_{shunt} (Ohms)	3.73E+04	3.73E+03	1.89E+04	1.99E+04
R_{series} (Ohms)	7.97E+01	6.53E+01	6.56E+01	7.02E+01

300µL SWCNTs +300µL MoS_2	Cell 1	Cell 2	Cell 3	Average

J_{sc} (mA/cm^2)	22.341	21.369	23.803	22.504
V_{oc}(V)	0.554	0.554	0.559	0.556
FF	0.65	0.71	0.63	0.66
Efficiency %	8.01	8.4	8.4	8.3
R_{shunt} (Ohms)	1.49E+04	7.98E+03	2.39E+04	1.56E+04
R_{series} (Ohms)	7.09E+01	5.78E+01	7.15E+01	6.67E+01

300µL SWCNTs +400µL MoS_2	Cell 1	Cell 2	Cell 3	Average
J_{sc} (mA/cm^2)	22.517	23.082	23.629	23.076
V_{oc}(V)	0.523	0.573	0.573	0.556
FF	0.63	0.63	0.63	0.63
Efficiency %	7.5	8.4	8.5	8.13
R_{shunt} (Ohms)	2.34E+04	4.34E+03	6.72E+03	1.15E+04
R_{series} (Ohms)	7.12E+01	8.07E+01	8.01E+01	7.73E+01

300µL SWCNTs +500µL MoS_2	Cell 1	Cell 2	Cell 3	Average
J_{sc} (mA/cm^2)	21.354	26.15	22.199	23.234
V_{oc} (V)	0.555	0.512	0.556	0.541
FF	0.66	0.64	0.7	0.67
Efficiency %	8.3	8.6	8.7	8.53
R_{shunt} (Ohms)	1.05E+04	1.08E+05	2.55E+04	4.80E+04
R_{series} (Ohms)	7.03E+01	5.60E+01	5.60E+01	6.1E+01

300µL SWCNTs +600µL MoS_2	Cell 1	Cell 2	Cell 3	Average
J_{sc} (mA/cm^2)	26.597	19.936	25.544	24.03
V_{oc} (V)	0.515	0.503	0.522	0.513
FF	0.61	0.64	0.61	0.62
Efficiency %	8.41	8.7	9.76	9
R_{shunt} (Ohms)	4.64E+03	2.10E+04	7.57E+03	1.11E+04
R_{series} (Ohms)	6.21E+01	7.13E+01	5.84E+01	6.39E+01

300µL SWCNTs +700µL MoS_2	Cell 1	Cell 2	Cell 3	Average
J_{sc} (mA/cm^2)	22.749	22.767	22.743	22.753
V_{oc} (V)	0.575	0.575	0.575	0.575
FF	0.7	0.71	0.71	0.71
Efficiency %	9.11	9.26	9.33	9.23
R_{shunt} (Ohms)	7.48E+03	6.66E+03	3.80E+03	5.98E+03
R_{series} (Ohms)	5.95E+01	5.93E+01	5.91E+01	5.93E+01

300µL SWCNTs +800µL MoS_2	Cell 1	Cell 2	Cell 3	Average
J_{sc} (mA/cm^2)	22.811	21.854	22.771	22.479
V_{oc} (V)	0.569	0.569	0.574	0.571
FF	0.61	0.65	0.69	0.65
Efficiency %	7.96	8.04	8.99	8.33
R_{shunt} (Ohms)	2.70E+03	7.62E+03	3.73E+03	4.68E+03
R_{series} (Ohms)	8.67E+01	8.72E+01	5.98E+01	7.79E+01

300µL SWCNTs +900µL MoS_2	Cell 1	Cell 2	Cell 3	Average
J_{sc} (mA/cm^2)	22.542	22.677	22.62	22.613
V_{oc}(V)	0.549	0.551	0.548	0.549
FF	0.65	0.66	0.68	0.66
Efficiency %	8	8.2	8.37	8.2
R_{shunt} (Ohms)	5.96E+03	1.82E+03	4.53E+03	4.1E+03
R_{series} (Ohms)	5.27E+01	5.47E+01	5.17E+01	5.3E+01

300µL SWCNTs +1000µL MoS_2	Cell 1	Cell 2	Cell 3	Average
J_{sc} (mA/cm^2)	22.48	22.402	20.55	21.81
V_{oc} (V)	0.548	0.549	0.57	0.56
FF	0.56	0.58	0.7	0.61
Efficiency %	6.95	7.09	8.15	7.4
R_{shunt} (Ohms)	1.59E+03	1.79E+04	2.41E+04	1.5E+04
R_{series} (Ohms)	1.14E+02	1.13E+02	7.16E+01	3.13E+01

300µL SWCNTs +2mL MoS_2	Cell 1	Cell 2	Cell 3	Average
J_{sc} (mA/cm^2)	18.976	19.39	19.031	19.13
V_{oc} (V)	0.534	0.557	0.554	0.548
FF	0.68	0.68	0.73	0.70
Efficiency %	6.93	7.29	7.65	7.3
R_{shunt} (Ohms)	7.79E+03	3.32E+04	4.62E+04	2.91E+04
R_{series} (Ohms)	5.43E+01	7.54E+01	5.33E+01	6.1E+01

Table (A3): this table shows the average sheet resistivity for the hybrid MoS_2/SWCNTs with the same films thickness (2 % HF etching experiment).

Sheet Resistivity ($\Omega.cm^{-1}$)				
Cell Name	Reading 1	Reading 2	Reading 3	Average Reading
300 µL SWCNTs	185	187	188	187
300µL SWCNTs+400µL MoS_2 (1)	361.1	378	388.3	376
300µL SWCNTs+400µL MoS_2 (2)	293.3	380	380.2	351.2
300µL SWCNTs+400µL MoS_2 (3)	285	302	304	297

Table (A4): The average parameters for the hybrid MoS_2/SWCNTs with the normal 2% HF etching time (15 seconds) solar cells.

300µL SWCNTs +400µL MoS_2	Cell 1	Cell 2	Cell 3	Average
J_{sc} (mA/cm^2)	22.517	24.556	24.177	23.75
V_{oc} (V)	0.523	0.524	0.573	0.54
FF	0.63	0.61	0.62	0.62
Efficiency %	8	8	8.62	8.04
R_{shunt} (Ohms)	2.34E+04	6.94E+03	6.54E+03	1.23E+04
R_{series} (Ohms)	7.12E+01	7.55E+01	8.12E+01	7.60E+01

Table (A5): The average parameters for the hybrid MoS_2/SWCNTs with different time 2% HF etching treatments more 15 second for cell (1), 30 second for cell (2) and 45 seconds solar cells.

300µL SWCNTs +400µL MoS_2	Cell 1	Cell 2	Cell 3	Average
J_{sc} (mA/cm^2)	21.553	23.292	21.683	22.176
V_{oc} (V)	0.527	0.533	0.526	0.529
FF	0.62	0.57	0.6	0.6
Efficiency %	7.6	7	6.5	7.03
R_{shunt} (Ohms)	4.04E+03	3.32E+03	1.37E+03	2.91E+04
R_{series} (Ohms)	6.27E+01	7.50E+01	7.80E+01	7.19E+01

Table (A6): The average sheet resistivity for the hybrid MoS_2/SWCNTs with different films thickness.

Sheet Resistivity ($\Omega.cm^{-1}$)				
Cell Name	Reading 1	Reading 2	Reading 3	Average Reading
300µL SWCNTs	185	188	192	188.3
150µL SWCNTs+200µL MoS_2	708	708.1	708.2	708.1
300µL SWCNTs+400µL MoS_2	412.2	437	459.2	436.1
600µL SWCNTs+800µL MoS_2	150	166	188.4	168.1
900µL SWCNTs+1200µL MoS_2	105	107.1	108	107
1200µL SWCNTs+1500µL MoS_2	71	78	78	76
1500µL SWCNTs+1800µL MoS_2	49.4	50	51.24	50.2

Table (A7): The average parameters for the hybrid MoS_2/SWCNTs with different thickness films filtrations solar cells

150µL SWCNTs +200µL MoS_2	Cell 1	Cell 2	Cell 3	Average
J_{sc} (mA/cm^2)	25.841	25.522	26.497	25.953
V_{oc} (V)	0.544	0.551	0.551	0.549
FF	0.35	0.36	0.35	0.35
Efficiency %	4.9	5.01	5.2	5.04
R_{shunt} (Ohms)	7.50E+02	1.00E+03	7.69E+02	8.40E+02
R_{series} (Ohms)	2.04E+02	1.90E+02	1.90E+02	1.95E+02

300µL SWCNTs +400µL MoS_2	Cell 1	Cell 2	Cell 3	Average
J_{sc}(mA/cm^2)	23.292	23.562	26.38	24.41
V_{oc} (V)	0.533	0.521	0.487	0.514
FF	0.61	0.62	0.67	0.63
Efficiency %	7.6	7.6	8.7	8
R_{shunt} (Ohms)	3.32E+04	6.33E+03	1.16E+04	1.70E+04
R_{series} (Ohms)	7.50E+01	7.70E+01	4.95E+01	6.72E+01

600µL SWCNTs +800µL MoS_2	Cell 1	Cell 2	Cell 3	Average
J_{sc} (mA/cm^2)	16.821	18.42	17.489	17.577
V_{oc} (V)	0.511	0.472	0.516	0.499
FF	0.7	0.69	0.69	0.69
Efficiency %	6	6.01	6.24	6.08
R_{shunt} (Ohms)	9.37E+03	8.69E+03	6.87E+04	8.31E+03
R_{series} (Ohms)	6.97E+01	5.55E+01	6.90E+01	6.47E+01

900µL SWCNTs +1200µL MoS_2	Cell 1	Cell 2	Cell 3	Average
J_{sc} (mA/cm^2)	11.047	10.469	11.846	11.121
V_{oc} (V)	0.541	0.522	0.545	0.536
FF	0.65	0.63	0.65	0.64
Efficiency %	3.9	4	4.2	4.03
R_{shunt} (Ohms)	2.68E+04	2.13E+04	1.63E+04	2.15 E+04
R_{series} (Ohms)	1.43E+02	1.54E+02	1.41E+02	1.46E+02

1200µL SWCNTs +1500µL MoS_2	Cell 1	Cell 2	Cell 3	Average
J_{sc}(mA/cm^2)	8.436	8.305	8.516	8.419
V_{oc}(V)	0.45	0.468	0.451	0.456
FF	0.7	0.69	0.71	0.7
Efficiency %	2.64	2.7	2.73	2.69
R_{shunt} (Ohms)	1.98E+04	2.87E+04	6.02E+04	3.62E+04
R_{series} (Ohms)	1.32E+02	1.15E+02	7.73E+01	1.08E+02

1500µL SWCNTs +1800µL MoS_2	Cell 1	Cell 2	Cell 3	Average
J_{sc} (mA/cm^2)	5.928	6.287	6.05	6.08
V_{oc} (V)	0.467	0.413	0.47	0.45
FF	0.63	0.69	0.64	0.65
Efficiency %	1.8	1.8	1.81	1.80
R_{shunt} (Ohms)	2.01E+05	6.99E+04	2.28E+04	9.79E+04
R_{series} (Ohms)	2.01E+02	1.12E+02	2.00E+02	1.71E+02

Table (A8): The average sheet resistivity for the hybrid layers films MoS_2 then SWCNTs with different MoS_2 volume filtrations solar cells.

Sheet Resistivity ($\Omega.cm^{-1}$)				
Cell Name	Reading 1	Reading 2	Reading 3	Average Readings
300µL MoS_2	188	193	194	192
100µL MoS_2+300µL SWCNTs	282.1	282.5	282.9	282.5
200µL MoS_2+300µL SWCNTs	127	129.4	130.1	128.8
300µL MoS_2+300µL SWCNTs	149.7	156.9	166.9	157.8
400µL MoS_2+300µL SWCNTs	117.4	131.3	149.2	132.6
500µL MoS_2+300µL SWCNTs	174.1	177.9	183.2	178.4
600µL MoS_2+300µL SWCNTs	167	169.6	170.8	169.1
700µL MoS_2+300µL SWCNTs	188.4	189.3	194	191
800µL MoS_2+300µL SWCNTs	204.2	207	214	208.4
900µL MoS_2+300µL SWCNTs	204	212	215.4	210.4
1000µL MoS_2+300µL SWCNTs	280	281.3	288	283.1

Table (A9): The average parameters for the hybrid layers films MoS_2 then SWCNTs with different MoS_2 volume filtrations solar cells.

300 µL MoS_2	Cell 1	Cell 2	Cell 3	Average
J_{sc} (mA/cm^2)	0.001	-0.001	-0.001	0.0003
V_{oc} (V)	0.004	-0.007	-0.007	- 0.003
FF	-17.92	-4.74	-4.58	- 9.08
Efficiency %	0	0	0	0
R_{shunt} (Ohms)	7.80E+04	8.34E+04	8.51E+04	8.22E+04
R_{series} (Ohms)	7.80E+04	8.80E+04	8.92E+04	8.51E+04

100µL MoS_2 +300µLSWCNTs	Cell 1	Cell 2	Cell 3	Average
J_{sc}(mA/cm^2)	21.537	20.637	21.673	21.282
V_{oc} (V)	0.497	0.498	0.494	0.496
FF	0.63	0.67	0.65	0.59
Efficiency %	6.77	6.84	6.91	6.84
R_{shunt} (Ohms)	2.13E+04	1.04E+04	1.35E+05	5.56E+04
R_{series} (Ohms)	6.65E+01	6.62E+01	6.28E+01	6.52E+01

200µL MoS_2 +300µL SWCNTs	Cell 1	Cell 2	Cell 3	Average
J_{sc} (mA/cm^2)	21.222	21.802	22.203	21.742
V_{oc}(V)	0.559	0.561	0.567	0.562
FF	0.66	0.66	0.73	0.68
Efficiency %	7.84	8.11	9.19	8.4
R_{shunt} (Ohms)	1.94E+06	1.30E+04	1.44E+04	6.6E+05
R_{series} (Ohms)	7.81E+01	7.64E+01	4.97E+01	6.81E+01

300µL MoS_2+ 300µL SWCNTs	Cell 1	Cell 2	Cell 3	Average
J_{sc} (mA/cm^2)	21.356	24.414	24.207	23.326
V_{oc} (V)	0.539	0.531	0.532	0.534
FF	0.7	0.64	0.66	0.67
Efficiency %	8.11	8.3	8.6	8.34
R_{shunt} (Ohms)	1.20E+05	3.91E+03	3.10E+04	5.16E+04
R_{series} (Ohms)	4.77E+01	6.30E+01	6.27E+01	5.78E+01

400µL MoS_2 + 300µL SWCNTs	Cell 1	Cell 2	Cell 3	Average
J_{sc}(mA/cm^2)	22.879	22.872	23.206	22.986
V_{oc} (V)	0.558	0.57	0.572	0.567
FF	0.6	0.73	0.72	0.68
Efficiency %	8	9.5	9.56	9.03
R_{shunt} (Ohms)	6.99E+03	4.00E+03	3.40E+06	1.15E+04
R_{series} (Ohms)	1.06E+02	5.04E+01	5.14E+01	7.73E+01

500µL MoS_2+ 300µL SWCNTs	Cell 1	Cell 2	Cell 3	Average
J_{sc}(mA/cm^2)	22.131	23.293	23.838	23.087
V_{oc} (V)	0.561	0.563	0.565	0.563
FF	0.72	0.72	0.71	0.72
Efficiency %	8.9	9.41	9.52	9.28

R_{shunt} (Ohms)	6.89E+03	7.42E+04	2.07E+04	3.39E+04
R_{series} (Ohms)	5.30E+01	4.87E+01	5.24E+01	5.14E+01

600µL MoS_2 + 300µL SWCNTs	Cell 1	Cell 2	Cell 3	Average
J_{sc} (mA/cm^2)	22.72	23.663	23.841	23.408
V_{oc} (V)	0.573	0.575	0.575	0.574
FF	0.74	0.75	0.74	0.74
Efficiency %	9.7	10.14	10.2	10.01
R_{shunt} (Ohms)	1.57E+04	2.92E+04	4.95E+03	1.67E+04
R_{series} (Ohms)	3.69E+01	3.66E+01	3.66E+01	3.67E+01

700µL MoS_2 + 300µLSWCNTs	Cell 1	Cell 2	Cell 3	Average
J_{sc} (mA/cm^2)	23.388	23.22	23.144	23.251
V_{oc}(V)	0.552	0.554	0.555	0.554
FF	0.72	0.73	0.74	0.73
Efficiency %	9.25	9.43	9.5	9.4
R_{shunt} (Ohms)	7.94E+03	4.95E+03	2.75E+04	1.35E+04
R_{series} (Ohms)	4.56E+01	4.69E+01	4.64E+01	4.63E+01

800µL MoS_2 + 300µL SWCNTs	Cell 1	Cell 2	Cell 3	Average
J_{sc}(mA/cm^2)	24.048	22.899	23.894	23.614
V_{oc} (V)	0.551	0.553	0.553	0.552
FF	0.61	0.71	0.7	0.673
Efficiency %	8.05	9.03	9.3	8.8
R_{shunt} (Ohms)	1.57E+04	6.38E+03	9.01E+03	1.04E+04
R_{series} (Ohms)	3.69E+01	9.79E+01	4.58E+01	6.02E+01

900µL MoS_2 + 300µL SWCNTs	Cell 1	Cell 2	Cell 3	Average
J_{sc} (mA/cm^2)	22.665	22.299	22.762	22.575
V_{oc} (V)	0.52	0.533	0.535	0.529
FF	0.58	0.67	0.68	0.64
Efficiency %	6.83	7.95	8.24	7.7
R_{shunt} (Ohms)	4.10E+03	5.85E+03	5.06E+04	5.0E+03
R_{series} (Ohms)	1.14E+02	6.38E+01	6.42E+01	8.1E+01

1000µL MoS_2 +300µLSWCNTs	Cell 1	Cell 2	Cell 3	Average
J_{sc} (mA/cm^2)	23.2	22.857	21.609	22.555
V_{oc} (V)	0.456	0.456	0.533	0.482
FF	0.62	0.63	0.68	0.64
Efficiency %	6.54	6.59	7.87	7
R_{shunt} (Ohms)	1.01E+04	2.07E+03	4.51E+03	5.56E+03
R_{series} (Ohms)	5.90E+01	5.81E+01	6.43E+01	6.05E+01